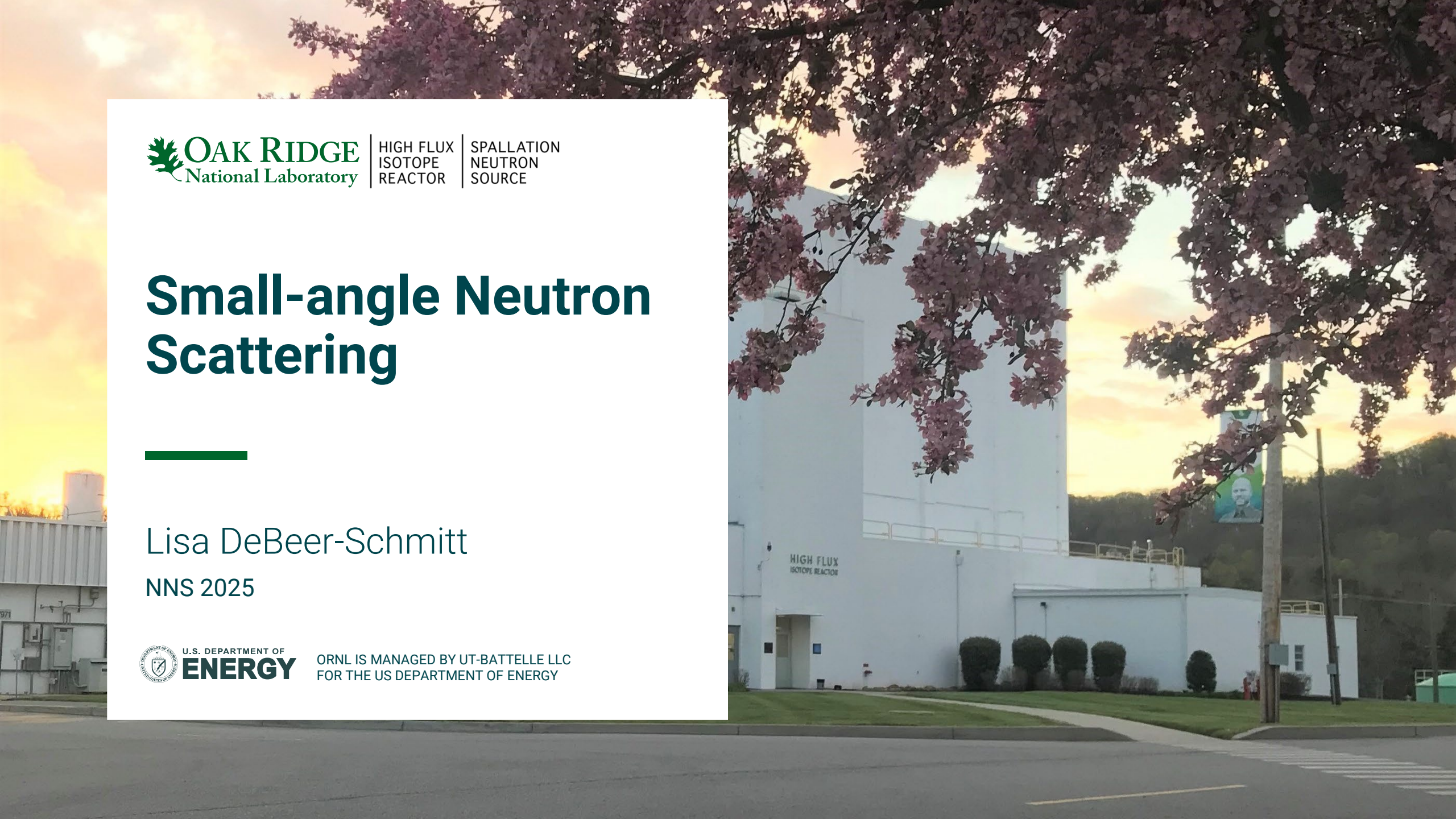

OAK RIDGE National Laboratory | HIGH FLUX ISOTOPE REACTOR | SPALLATION NEUTRON SOURCE

Small-angle Neutron Scattering

Lisa DeBeer-Schmitt

NNS 2025

U.S. DEPARTMENT OF ENERGY

ORNL IS MANAGED BY UT-BATTELLE LLC
FOR THE US DEPARTMENT OF ENERGY

A little about my career…

2008

Ph.D. at University of Notre Dame

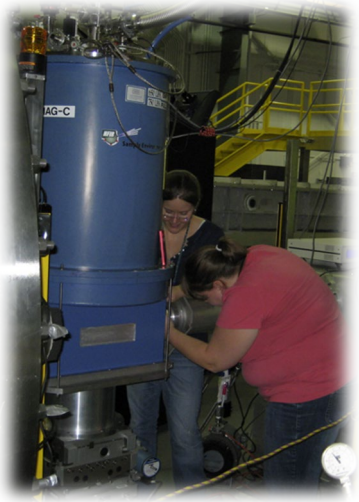

2009 - 2010

Post-doc at GP-SANS

2010 - 2011

Team Lead for SNS Sample Environment

2011 – 2015

Scientific Associate for Sequoia

2015 - current

Point-of-contact for GP-SANS

Outline:

- What is SANS?
- Instruments at ORNL
- Sample Environment capabilities
- Science Cases
  - Polymers
  - Magnetic ordering (diffraction)
  - Engineering materials
- New Directions

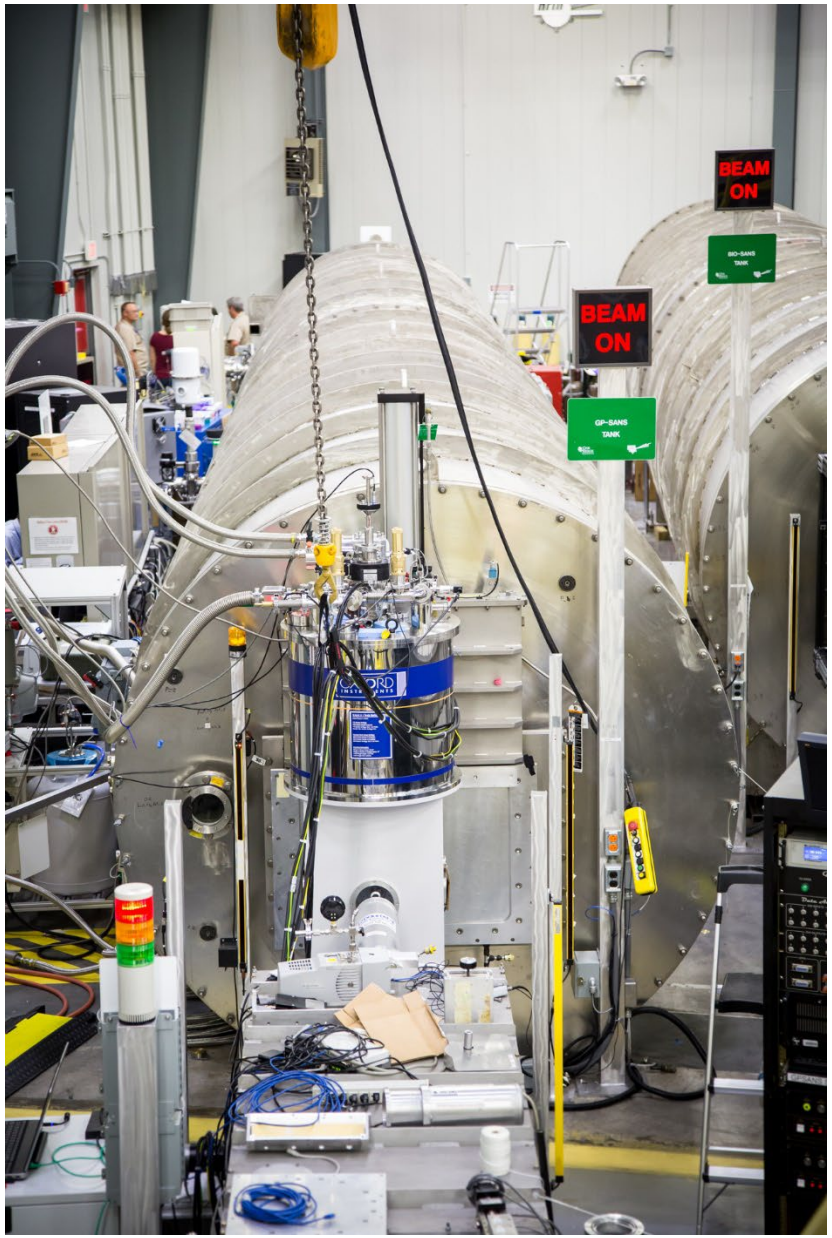

Small-angle neutron scattering (SANS)

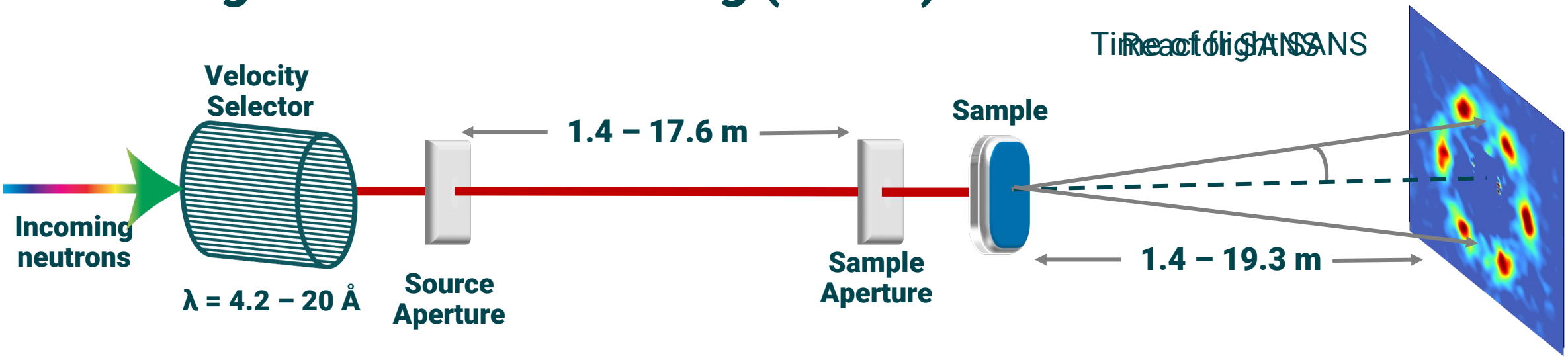

Scattering length density

Volume fraction

$$I(Q) = A\ \Delta\rho^2\ n\ V^2\ P(Q)\ S(Q)$$

Calibration

Number of scatters

Form and structure factors

Probes lengths of 0.5 – 700 nm
Using angles of θ= <0.1 to 45°

A powerful tool for studying nanophase bulk materials

Small-angle neutron scattering (SANS)

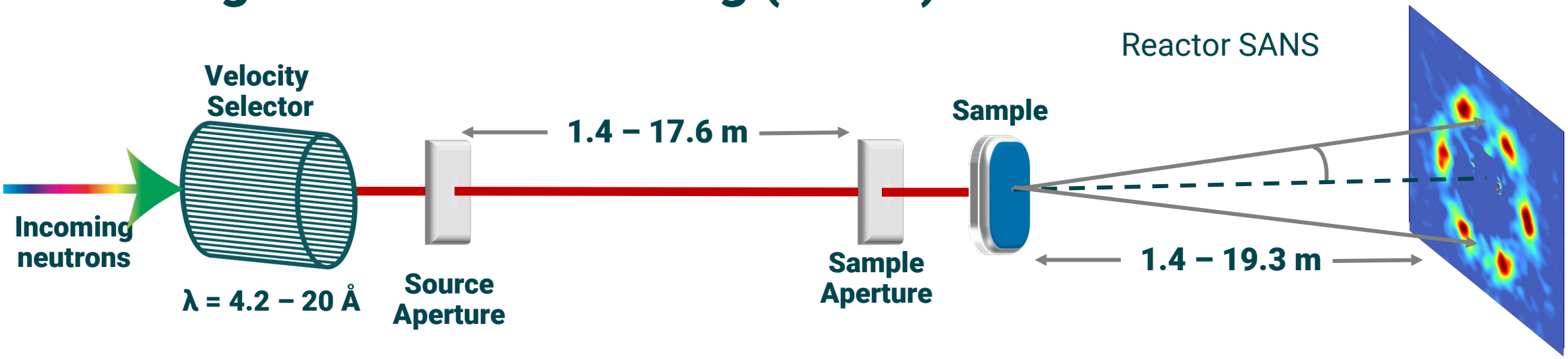

Q vs Real-space Length Scale in SANS

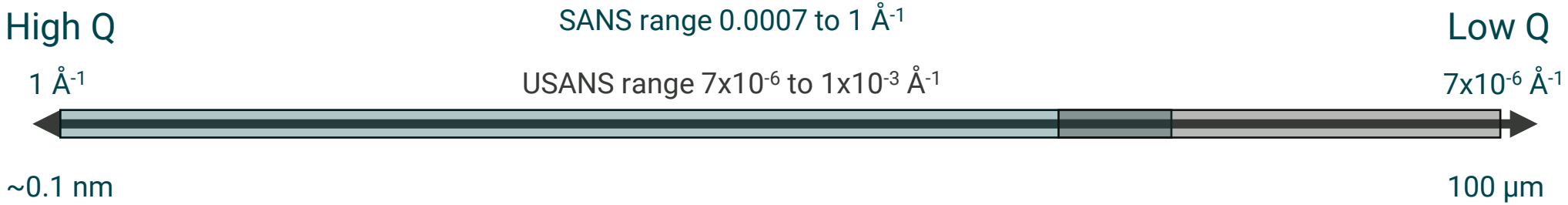

OAK RIDGE National Laboratory

A powerful tool for studying nanophase bulk materials

Why Neutrons?

- Low Energy (E=80meV for 1 Å neutrons vs. 12.42 keV for x-rays. **No radiation damage**.)
- High Penetration of cold neutrons – bulk samples
- Large difference in the scattering cross-section for the hydrogen and deuterium- contrast variation capability.
  - Solute or solvent can be deuterated to vary the contrast (ρ_{H2O} = -0.56x10^{10}cm^{-2}, ρ_{D2O} = 6.334x10^{10}cm^{-2})
  - Study of multicomponent systems through selective deuteration and contrast matching with H/D mixtures.
- Sensitive to substantial difference in scattering length density in transition metals
- MAGNETISM.
  - Neutron has a magnetic moment and spin which give contrast

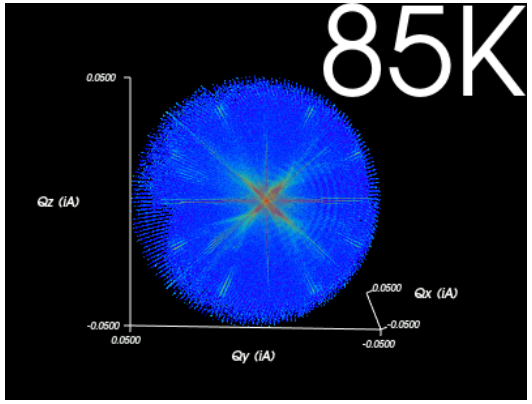

Magnetic domains in FeV_2O_4

L. Kish et al in preparation

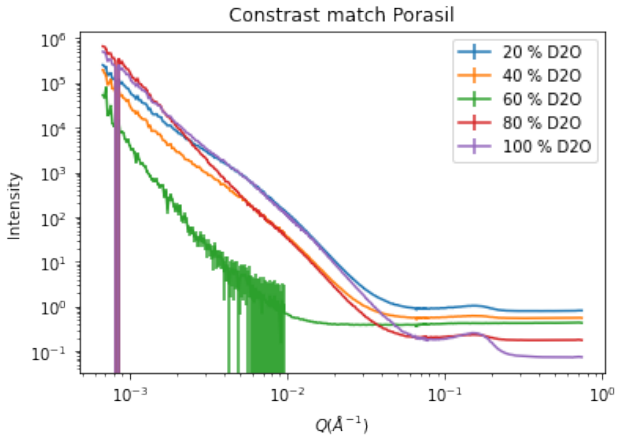

Data from NXschool experiment

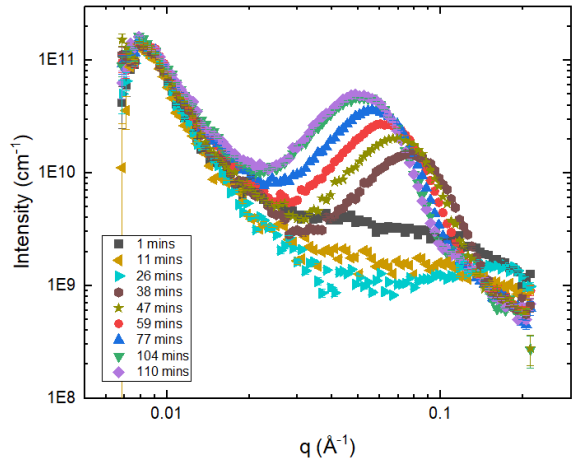

Copper precipitate growth in steel

SANS with other techniques

- Microscopy: Direct but limited

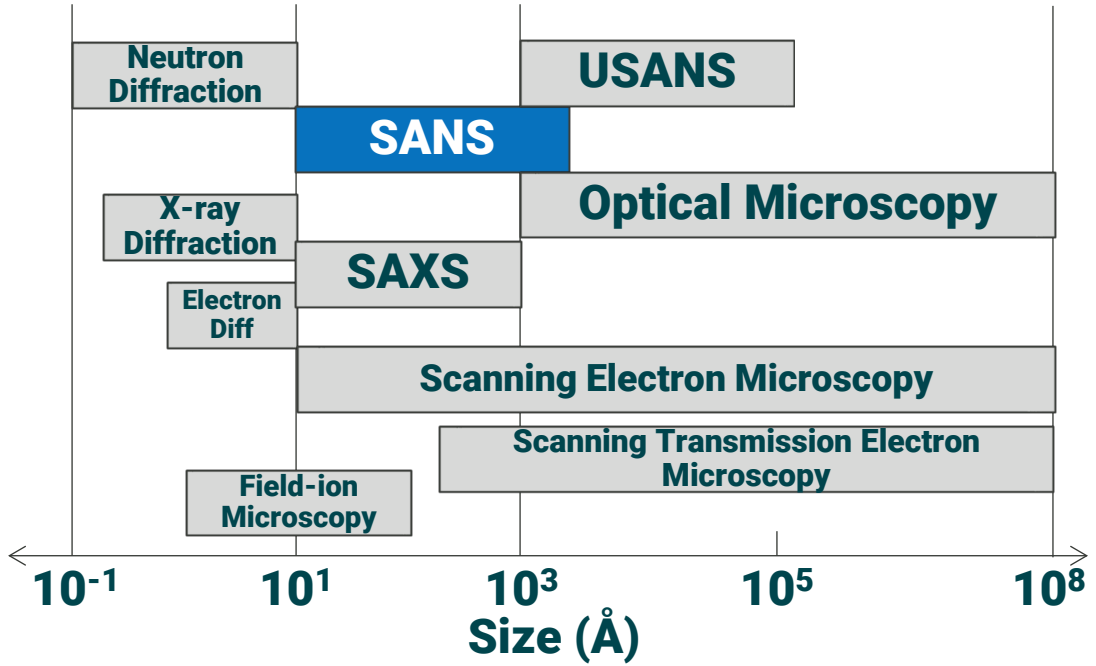

- SAS: Indirect and model-dependent but in-situ

SANS with other techniques

- Microscopy: Direct but limited

Finally discovered in 1981 and a second in 2003

- SAS: Indirect and model-dependent but in-situ

Neutron and x-ray scattering cross-sections

X-ray and neutron scattering are essentially the same concept, except...

- X-rays scatter from electrons

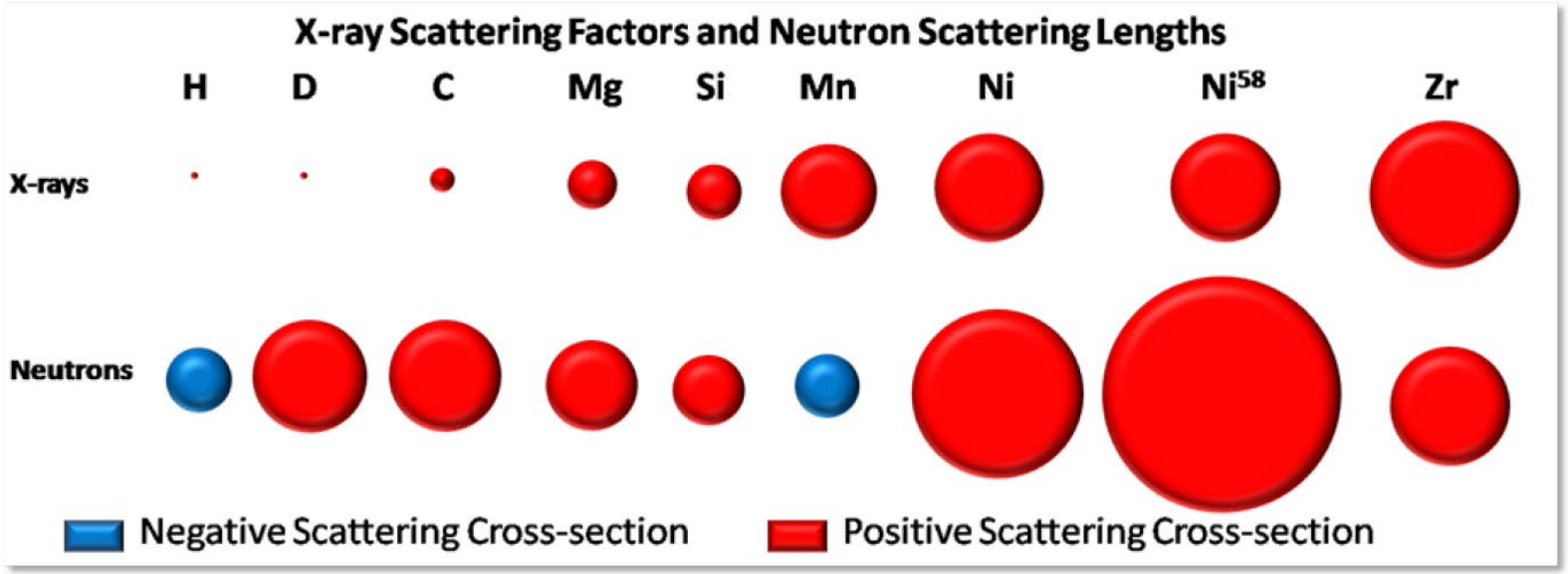

http://www.ncnr.nist.gov/resources/n-lengths/
http://www.isis.rl.ac.uk/ISISPublic/reference/Xray_scatfac.htm

C. Metting, Dissertation University of Maryland 2011

SANS from heirarchical structures

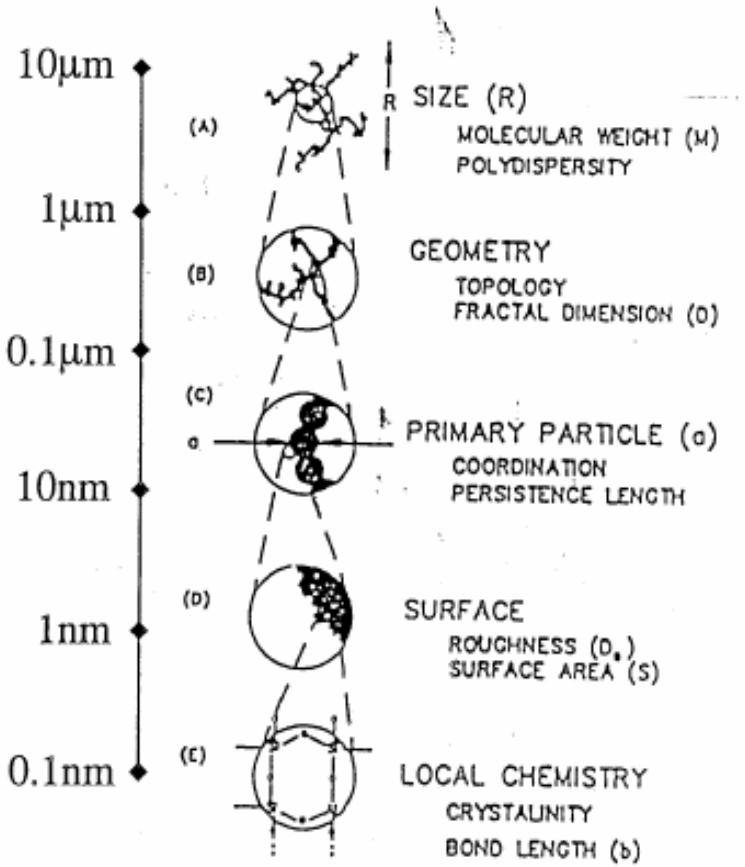

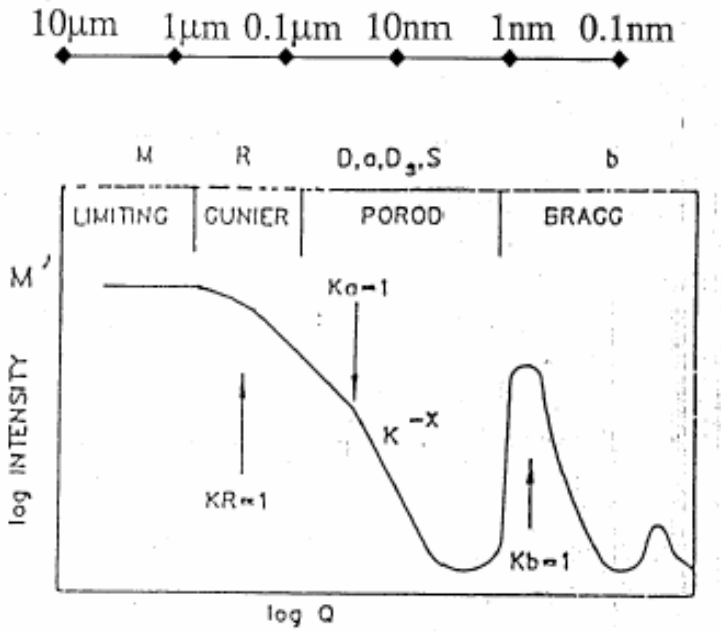

SANS is a structural technique that probes a wide array of length scales

SANS Suite

ORNL SANS instrument specifications.

	GP-SANS	Bio-SANS	EQ-SANS	USANS
Moderator	Supercritical hydrogen	Supercritical hydrogen	Coupled, supercritical hydrogen	Decoupled, poisoned hydrogen
Source	Reactor, continuous	Reactor, continuous	Spallation, 60 or 30 Hz, TOF	Spallation, 60 Hz, TOF
Sample-to-detector distance	1.1–20 m	1.1–15.5 m	1.0–9 m	N/A
Beam size	Up to 20 mm diameter	Up to 20 mm diameter	Up to 15 mm diameter	Up to 40 mm by 40 mm
Q range	7×10^{-4} to 1 Å^{-1}	9×10^{-4} to 1 Å^{-1}	2×10^{-3} to 6 Å^{-1}	7×10^{-6} to 5×10^{-3} Å^{-1}
Incident wavelength	4–25 Å	6–25 Å	0.5–20 Å	3.6, 1.8, 1.2 and 0.9 Å
$\Delta\lambda/\lambda$	9–45%	9–45%	<1–20%†	Monochromated with crystals
Detector type	^{3}He LPSD array	^{3}He LPSD array	^{3}He LPSD array	^{3}He

† The resolution of EQ-SANS is wavelength dependent and also depends on the binning used in the software. The upper end of the range indicated is for the shortest wavelength used in the current data reduction.

Sample Environments:

Current Sample environment options:

- New Robot sample changer
  - Peltier system that goes from -10 to 120 °C with 0.01 degree control and holds 42 samples at temperature
  - Atmosphere Furnace up to 300 °C
- Rheometer
- New controlled atmosphere furnace and vacuum furnace to > 1000 °C
- Horizontal 11 T recondensing magnet allowing users to utilize 11 T at 30 mK. (3/2016), 5 T horizontal open bore magnet (5/2017) and 8 T vertical magnet with temps 30 mK to 300 K
  - Electric field and current can also be applied to the samples
- SANS dedicated cryostat with sapphire windows
- Pressure cells (McHugh 2kBar and 1kBar changer)

Future upgrades:

- Strain cell to apply in-situ compression or tension (11 T and 5 T magnets)
- In-situ reaction vessel
- Load frame for metallurgical specimens

Science cases

Diblock copolymers

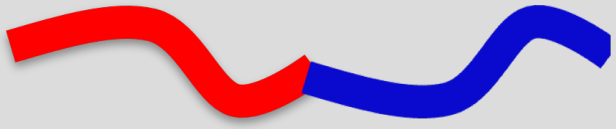

Skyrmion in thin films

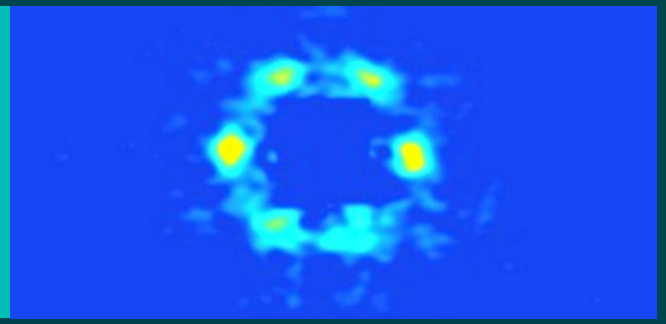

Novel Steels for reactor

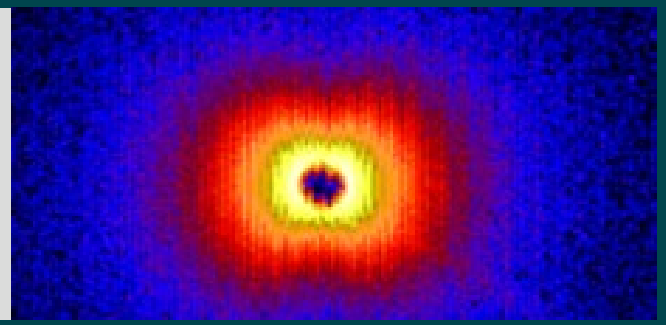

OAK RIDGE National Laboratory

Influence of Cleavage of Photosensitive Group on Micellization and Gelation of a Doubly Responsive Diblock Copolymer

Lilin He[1], Bin Hu[2], Daniel M. Henn[2], and Bin Zhao[2]

[1] Large Scale Structure Group, Neutron Scattering Division, Oak Ridge National Laboratory

[2] Department of Chemistry, University of Tennessee: Knoxville

Influence of Cleavage of Photosensitive Group on Micellization and Gelation of a Doubly Responsive Diblock Copolymer

Block Copolymers have wide technical applications owning to their capabilities to self-assemble into nanostructures under different conditions.

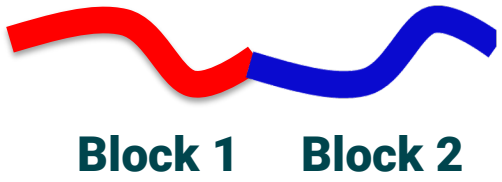

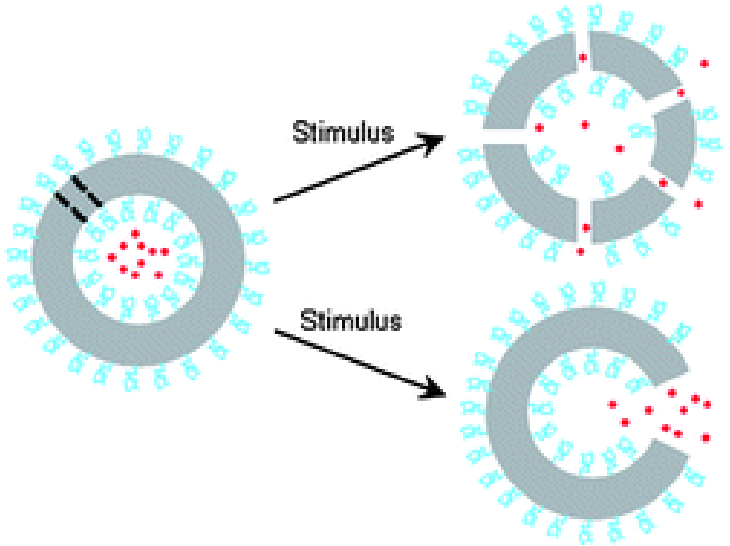

Controlled release example

Challenge: To precisely **tune** and **control** the molecular characteristics of the block copolymers under appropriate conditions.

Mark A. Ward, Theoni K. Georgiou, *Polymers* 2011, *3*(3), 1215-1242;

Thermal- and light-sensitive diblock copolymer PEO-b-P(TEGEA-co-NBA)

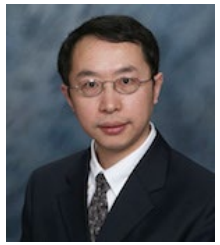

Prof. Bin Zhao, UTK

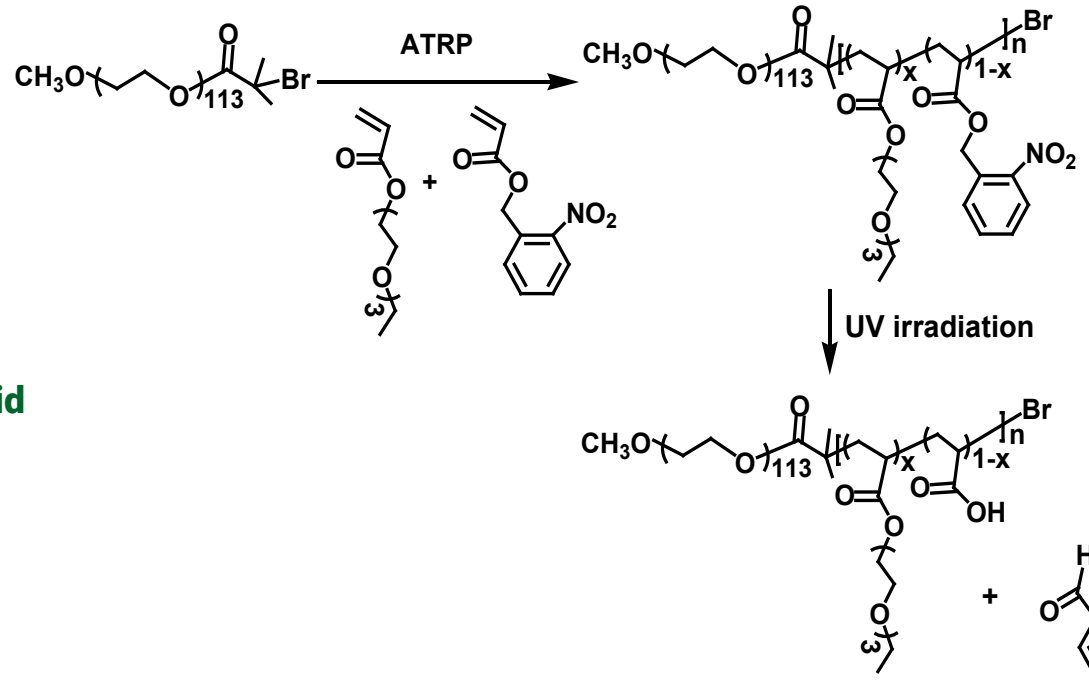

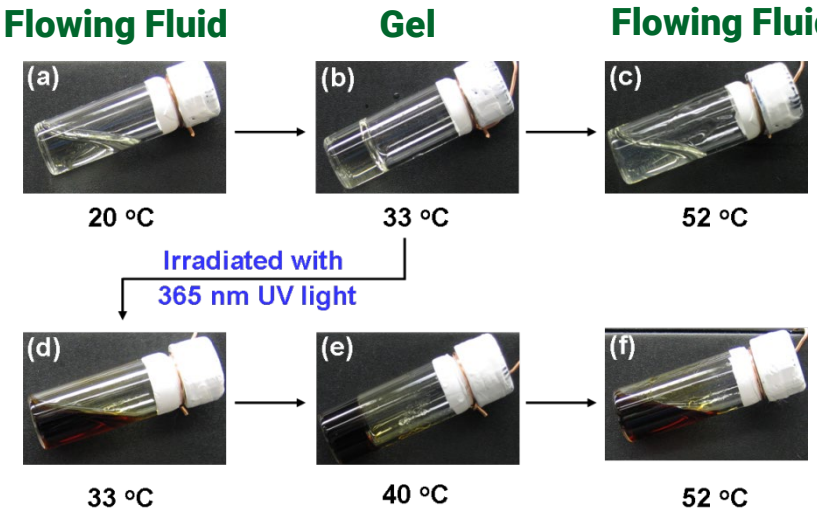

- "living"/controlled radical polymerization
- Irradiated for 6 days with 365nm UV light

- Brown-red color due to the photochemical reaction
- Multiple transitions

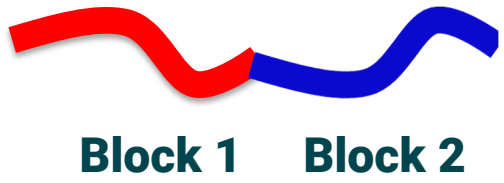

Jiang XG, et al. Macromolecules, 42, 8468-8476, 2009.

Rheological Results

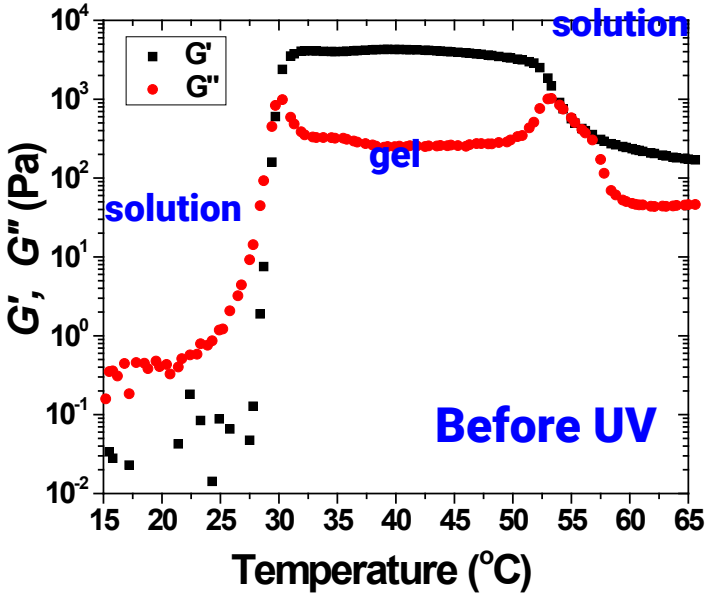

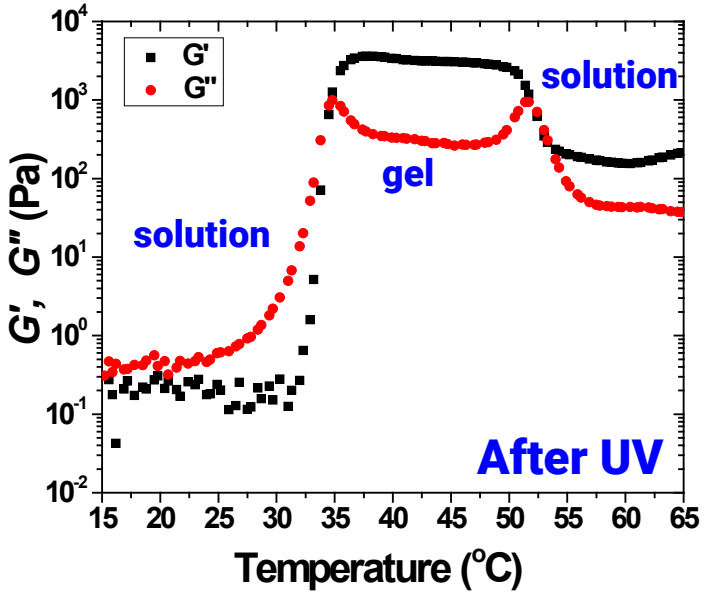

- Dynamic storage modulus *G'*, loss modulus *G"*, versus temperature
- 25wt % D_2O solution of PEO-*b*-P(TEGEA-*co*-NBA).
- A heating rate of 3°C/min.
- A strain amplitude of 1 %
- An oscillation frequency of 1 Hz.

- Reversible sol-gel-soft gel transitions is achieved;
- Gel is composed of packed micelles;
- UV irradiation leads to a narrower gel state window.

Rheological Properties ⟷ **Microstructure**

SANS results: Unimer State

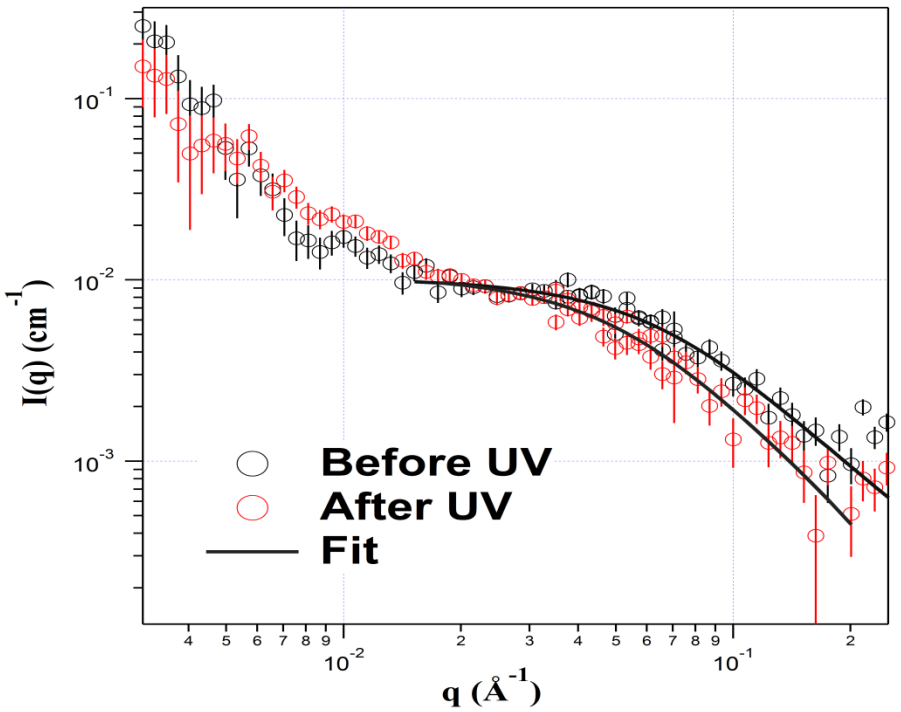

- Guinier Approximation at low-q:
  - $I(Q) = I(0) \exp(-Q^2R_g^2/3)$
  - $\ln[I(Q)]$ vs. Q^2 plot where $Q.R_g < 1.0$
  - $R_g = \sqrt{(3.\text{slope})}$
  - $M=(1000.I(0).d^2.Na)/(C.\Delta\rho^2)$
- Power-law at high q

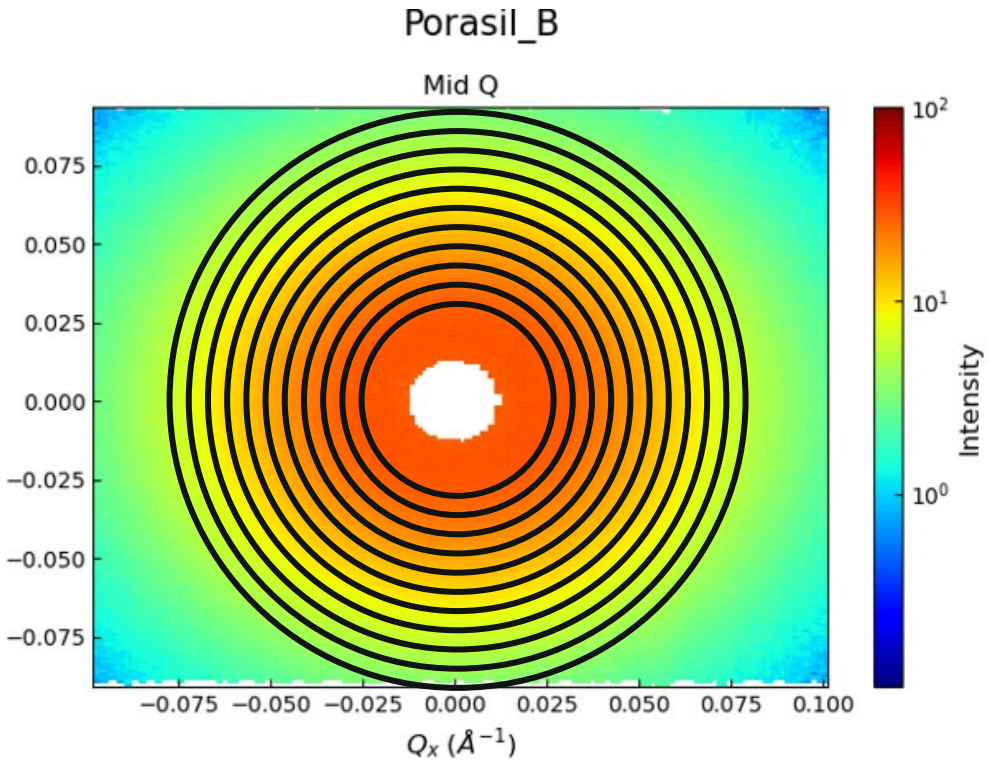

Lilin He, et al. **Polymer**, Volume 105, 25-34 (November 2016) https://doi.org/10.1016/j.polymer.2016.10.019

SANS results: Unimer State

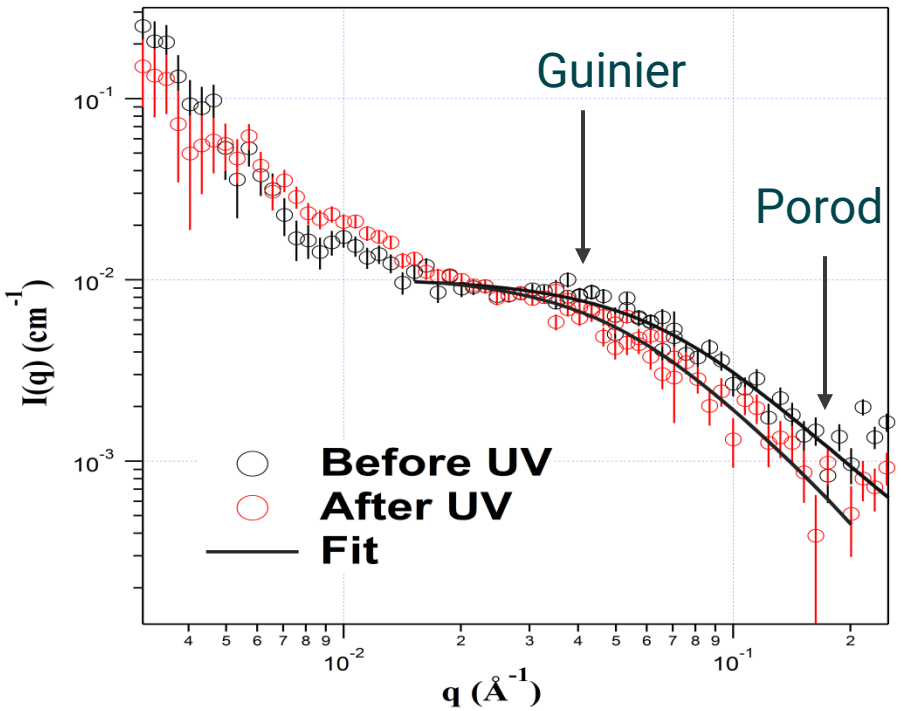

- Guinier Approximation at low-q:
  - $I(Q) = I(0) \exp(-Q^2R_g^2/3)$
  - $\ln[I(Q)]$ vs. Q^2 plot where $Q.R_g < 1.0$
  - $R_g = \sqrt{(3.\text{slope})}$
  - $M = (1000.I(0).d^2.Na)/(C.\Delta\rho^2)$
- Power-law at high q

Real Space

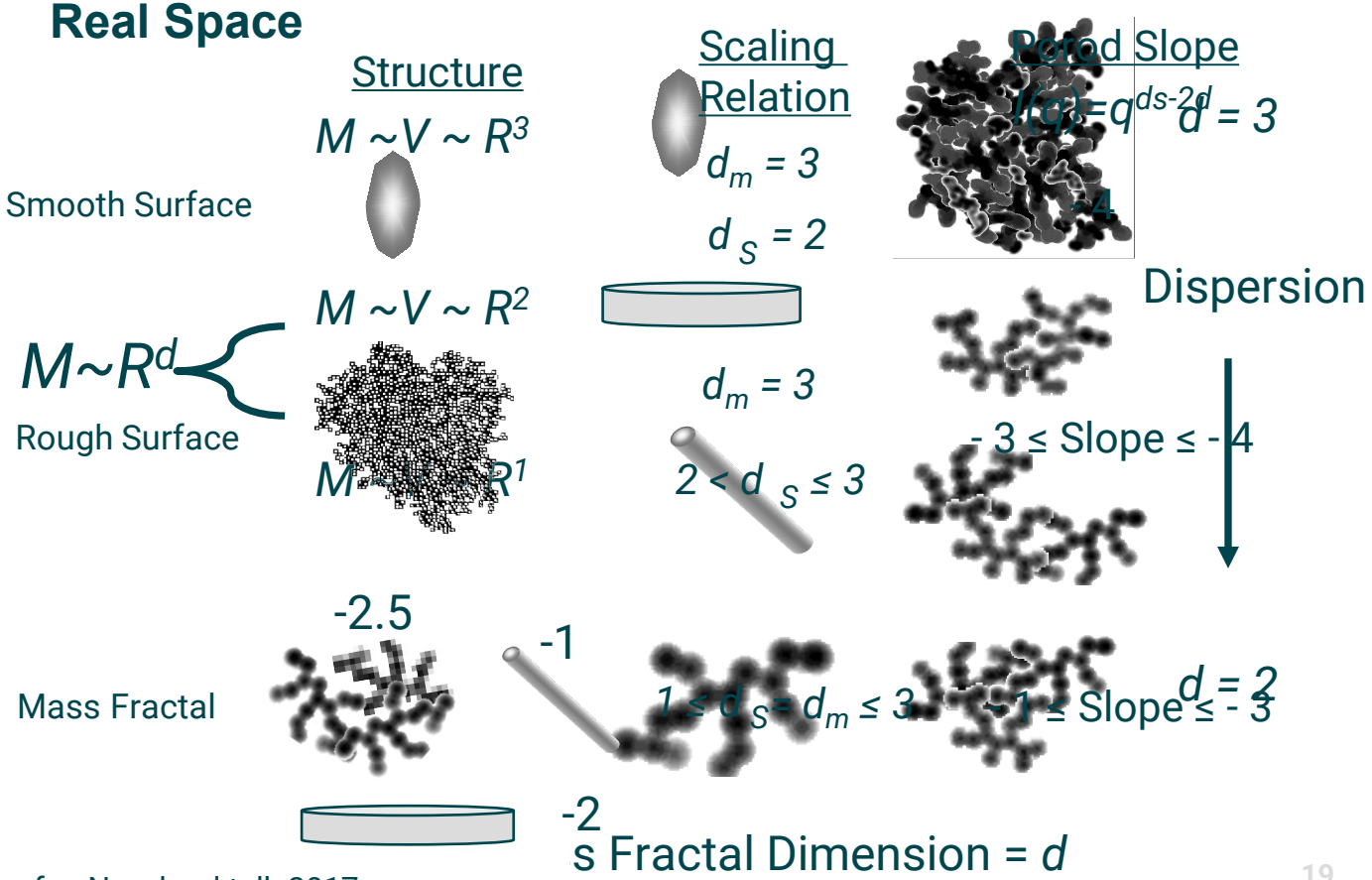

Lilin He, et al. **Polymer**, Volume 105, 25-34 (November 2016) https://doi.org/10.1016/j.polymer.2016.10.019

Dale Shaefer: Nxschool talk 2017

SANS results: Unimer State

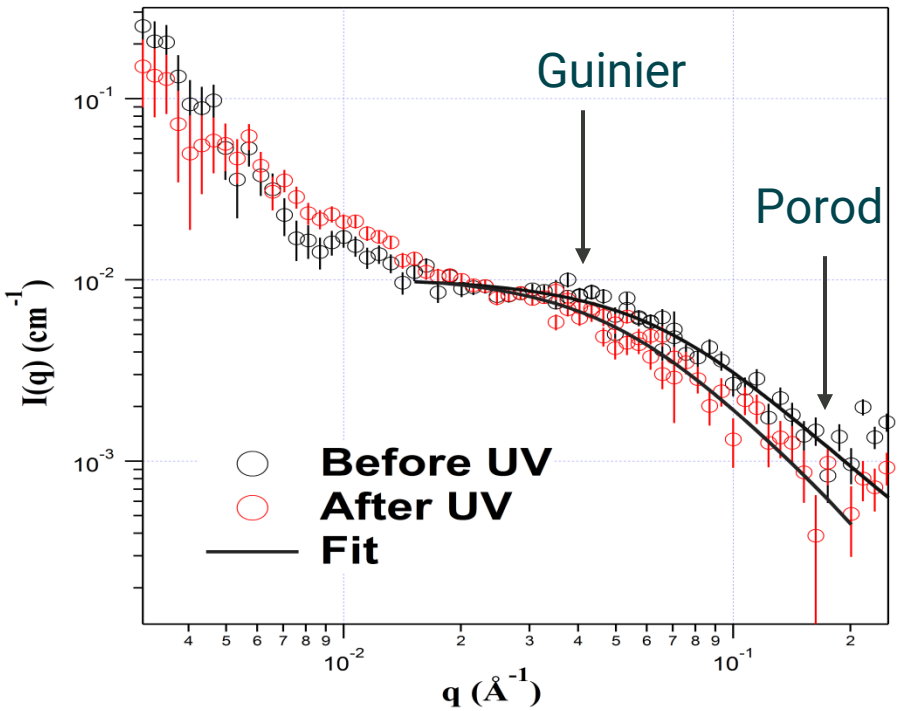

- ***0.02wt%***
- ***15 °C***

A model for polymers with excluded volume fraction yields Rg and Porod exponent

Before UV
R_g = 25.5Å
Porod exponent = 1.94

After UV
R_g = 31.1Å
Porod exponent = 1.59

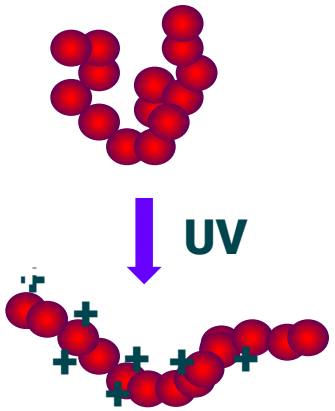

- ***Both solutions contain single chains and loosely-assembled clusters***
- ***The chains are more stretched after UV irradiation***

Lilin He, et al. **Polymer**, Volume 105, 25-34 (November 2016) https://doi.org/10.1016/j.polymer.2016.10.019

Temperature Effect: dilute solution

Before UV

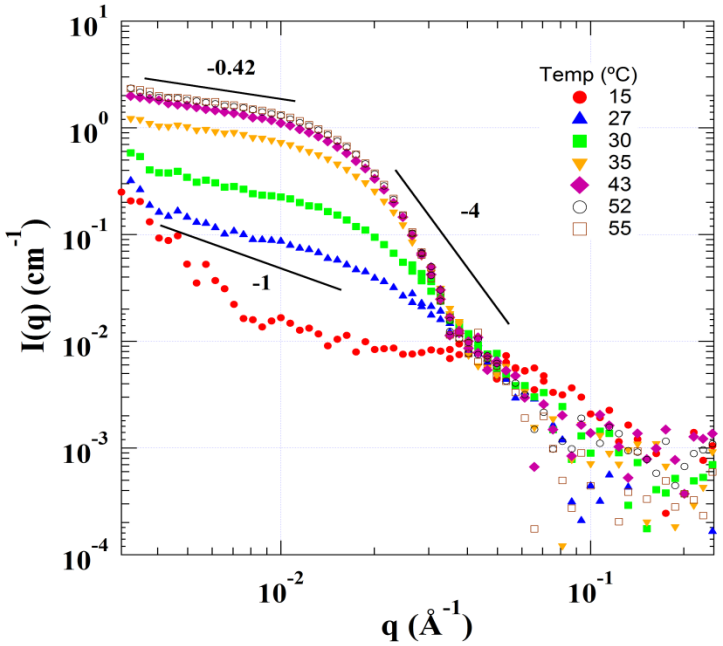

After UV

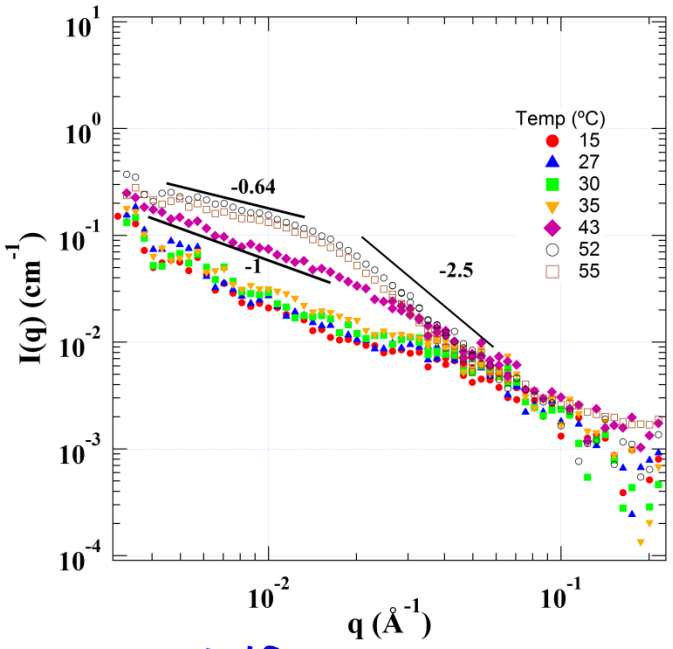

0.02wt%

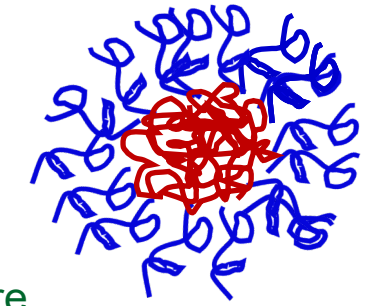

- Micelles form above critical micelle temperature
- Cleaving the light sensitive group defers the formation of the micelles

Lilin He, et al. **Polymer**, Volume 105, 25-34 (November 2016) https://doi.org/10.1016/j.polymer.2016.10.019

Temperature Effect: Concentrated solution

Before UV

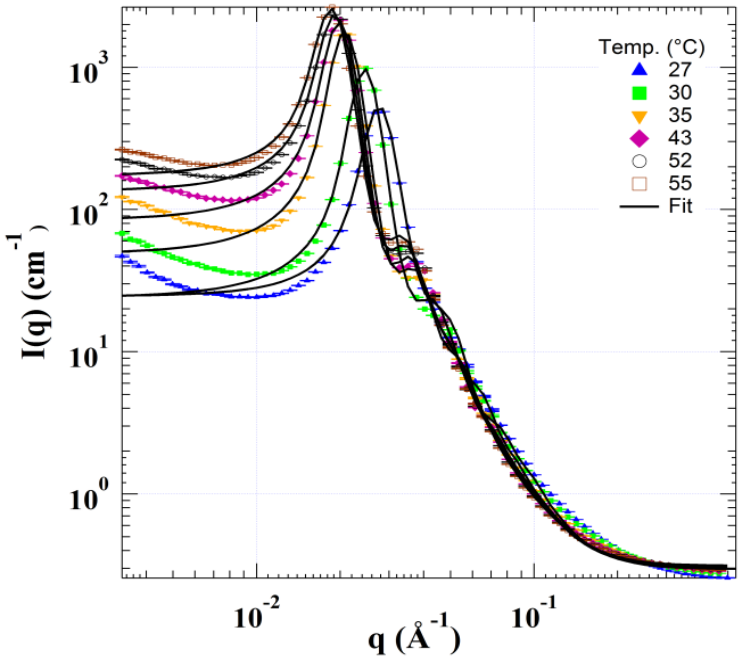

After UV

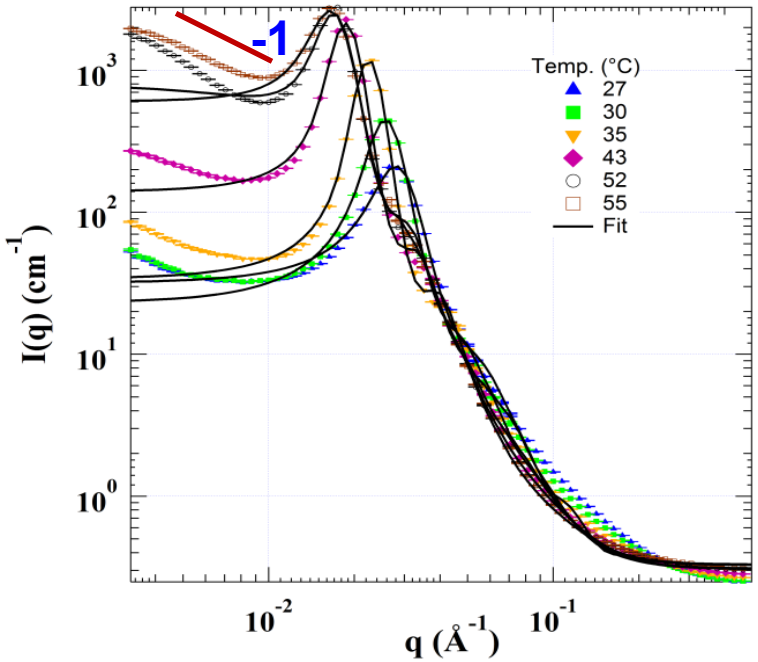

25 wt%

- Micelles grows with temperature;
- Possible sphere to rod transition at 55C for the UV exposed sample.

Lilin He, et al. **Polymer**, Volume 105, 25-34 (November 2016) https://doi.org/10.1016/j.polymer.2016.10.019

Model Fitting: Polycoreshell model

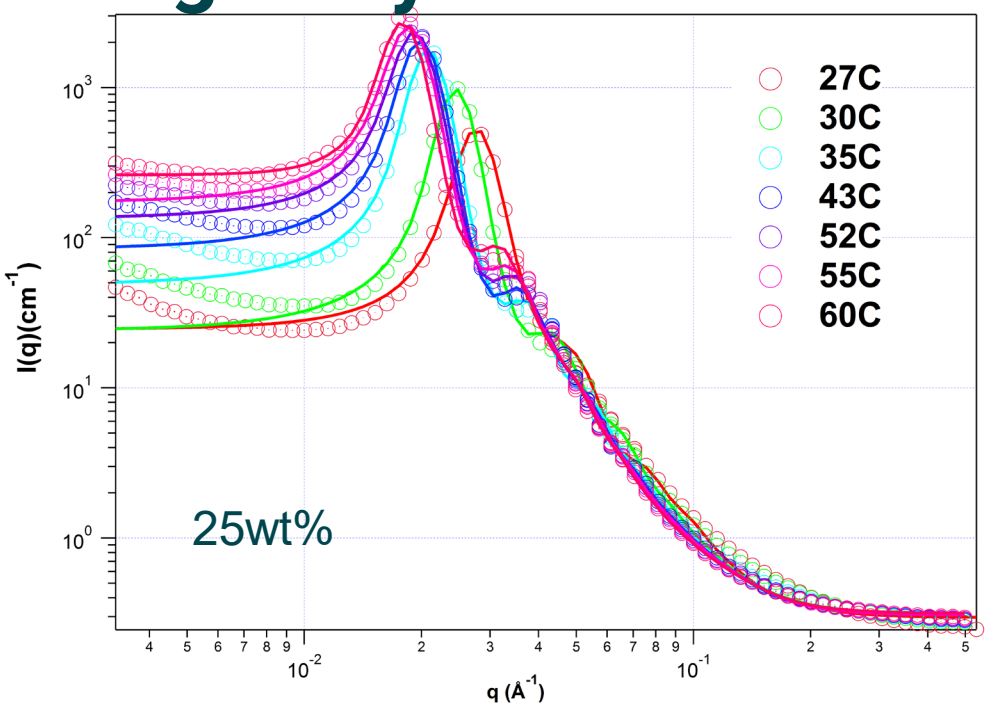

$$\frac{d\Sigma(Q)}{d\Omega} = \Delta\rho^2 \phi V_p P(Q) S(Q)$$

Percus-Yevick closure of the Ornstein-Zernike equation

Material Balance Calculation

$$N_{ag}(131*\nu_{TN}+113*\nu_{PEO}*f)+30*c = \frac{4\pi}{3} R_A{}^3$$

$$N_{ag}*113*\nu_{PEO}*(1-f)+30*d = \frac{4\pi}{3}(R_B{}^3 - R_A{}^3)$$

$$N_{ag}(131*b_{TN}+113*b_{PEO}*f)+191*c = \frac{4\pi}{3} R_A{}^3 * \rho_A$$

$$N_{ag}*113*b_{PEO}*(1-f)+191*d = \frac{4\pi}{3}(R_B{}^3 - R_A{}^3) * \rho_B$$

- **Micelle size (core and corona) and volume fraction**
- **Size polydispersity**
- **SLDs in core and corona**
- **Aggregation number**
- **Number of D_2O molecules in core and corona**
- **Fraction of PEO chains in core and corona**

J. B. Hayter in "Physics of Amphiphiles--Micelles, Vesicles, and Microemulsions" Eds. V. DeGiorgio; M. Corti, pp. 59-93,1983
B. Hammouda, "SANS from Pluronic P85 in d-water" European Polymer Journal, 46, 2275-2281, 2010.

Temperature Effect: Concentration solution

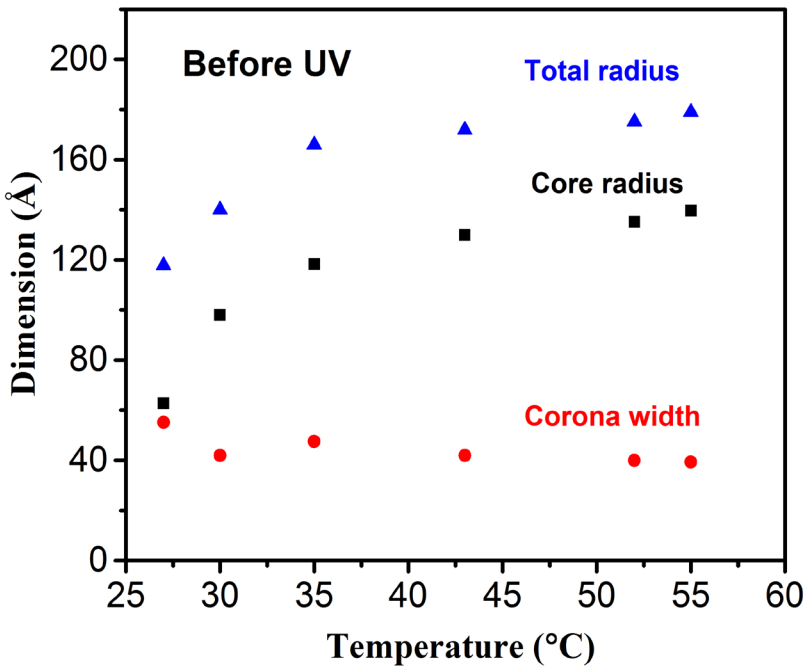

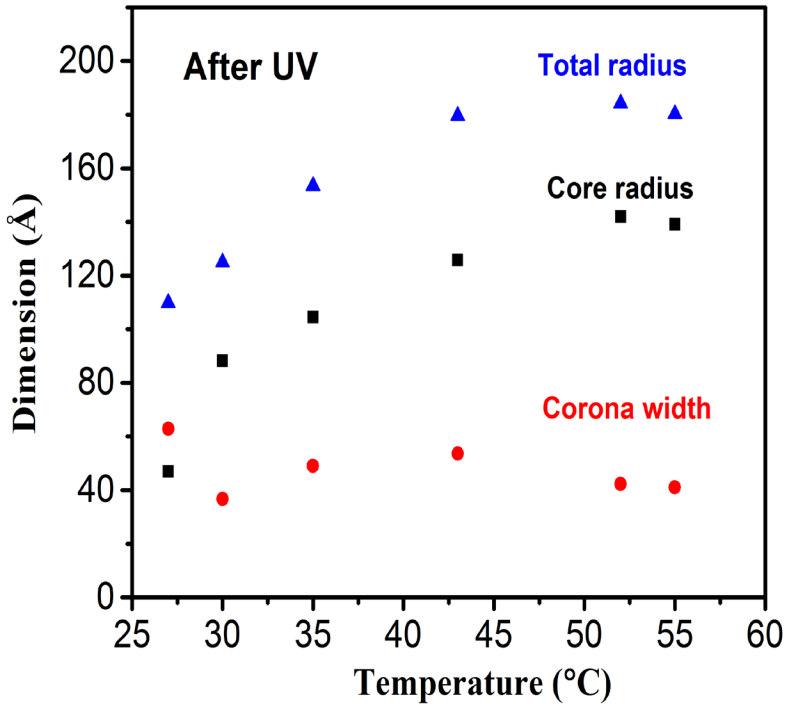

- The core size increases while the corona width remains;
- The slight shrinkage of corona at high temperatures is attributed to the loss of water, which is caused by the reduced miscibility of water and PEO.

Temperature dependence of particle volume fraction

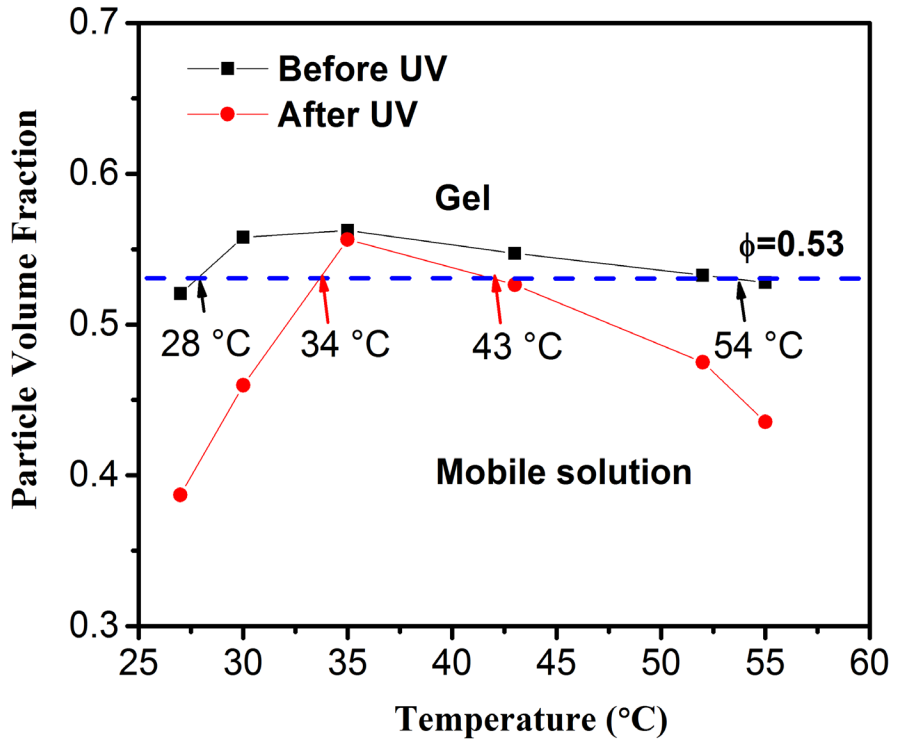

- Micelle effective volume fraction agrees the viscoelastic properties of solutions;
- Delayed gel formation in irradiated sample due to higher LCST transition;
- Critical value 0.53+/-0.02

Summary of Polymer Micellization

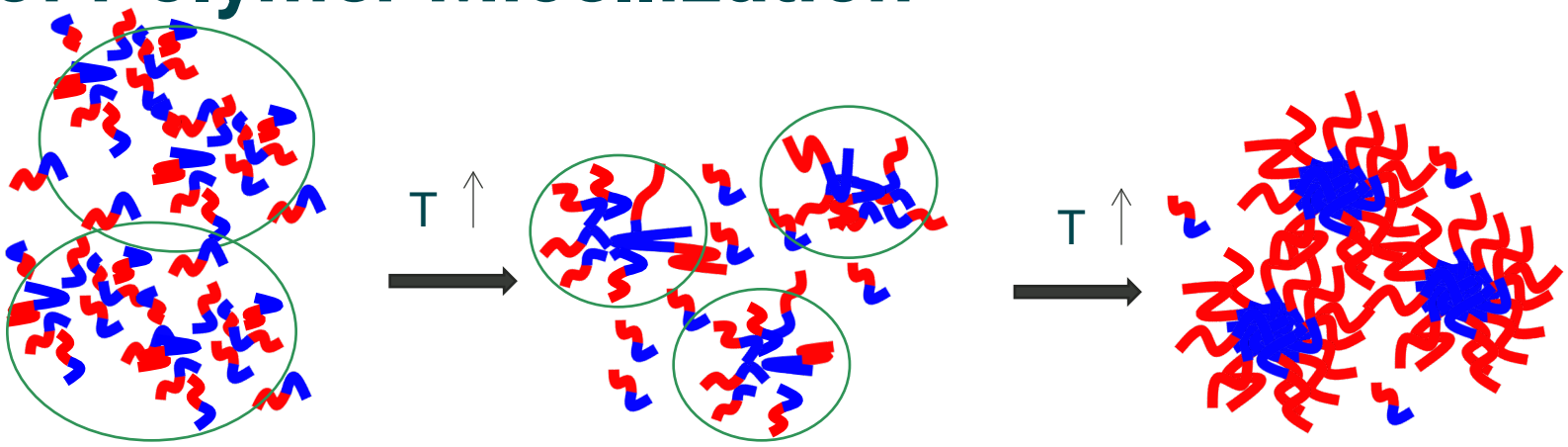

Unimers and clusters

Mixture of micelles and unimers

"well-defined" micelles
(Micellar solution)

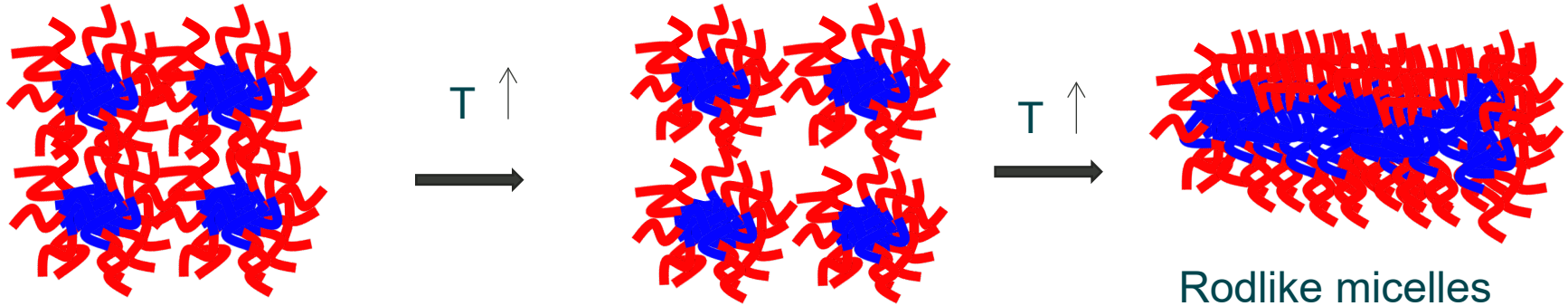

Ordered micelles
(Micellar gel)

Micellar solution
(Less overlapping and entangled chains)

Rodlike micelles
(for irradiated
sample only)

OAK RIDGE National Laboratory

Realization of magnetic skyrmions in thin films at ambient conditions

Ryan Desautels, **Lisa DeBeer-Schmitt**, Sergio Montoya, Julie Borchers, Soong-Guen Je, Nan Tang, Mi-Young Im, Micheal Fitzsimmons, Eric Fullerton, Dustin Gilbert

U.S. DEPARTMENT OF ENERGY

ORNL IS MANAGED BY UT-BATTELLE LLC
FOR THE US DEPARTMENT OF ENERGY

THE UNIVERSITY OF TENNESSEE KNOXVILLE

UC San Diego
JACOBS SCHOOL OF ENGINEERING

NIST Center for Neutron Research

SPAWAR

CXRO THE CENTER FOR X-RAY OPTICS

Skyrmions: a brief introduction

Tony Skyrme
Nuc. Phys. 13, 556 (1962)

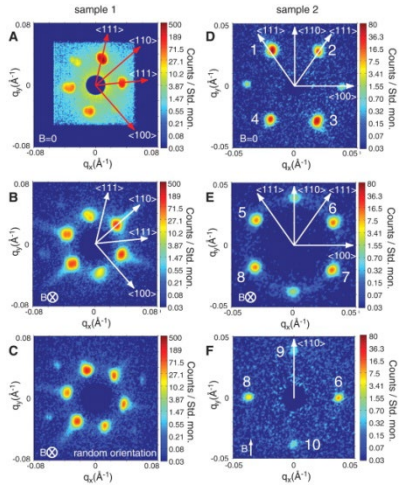

Science 323, 915 (2009)

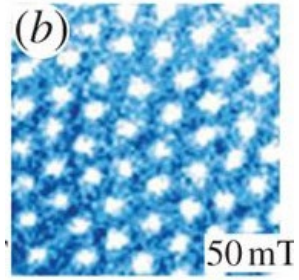

Nature 465, 901 (2010)

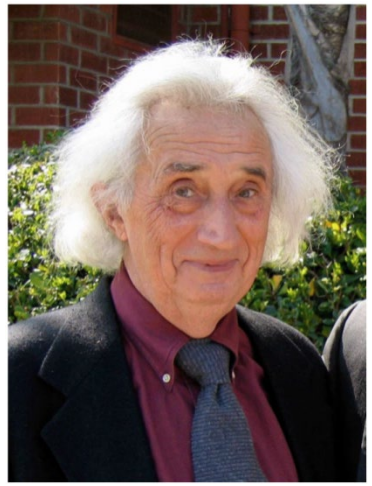

Igor Dzyaloshinskii
Soviet Physocs Jetp. 5, 1259 (1957)

Toru Moriya
Phys. Rev. 120, 91 (1960)

$$E \propto D(\vec{S}_1 \times \vec{S}_2)$$

DM Interaction Prefers 90° Orientation

Defines a 'handedness'

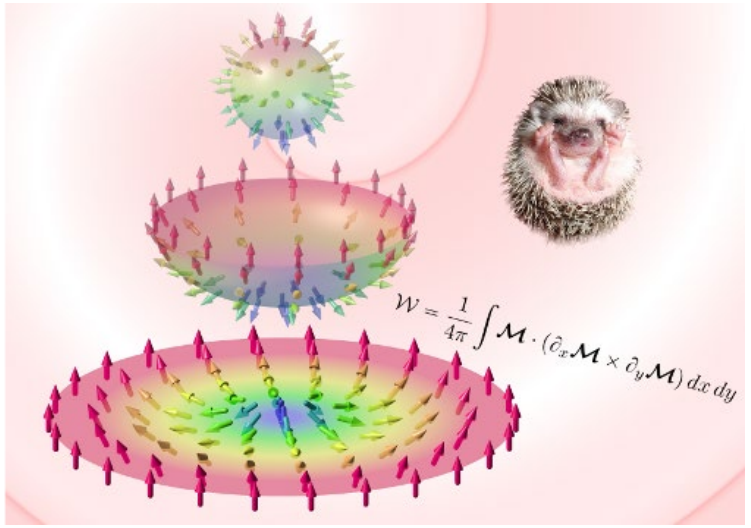

Predicted in magnetic systems
(Phys. Rev. Lett. 87, 037203 (2001))

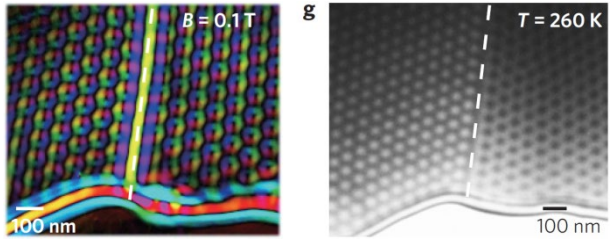

Nature Mater. 10, 106 (2011)

Direct Exchange Prefers Parallel Alignment

$$E \propto J(\vec{S}_1 \cdot \vec{S}_2)$$

OAK RIDGE National Laboratory

Skyrmions: a brief introduction

Néel (hedgehog)

Bloch

(arrows indicate magnetic spins)

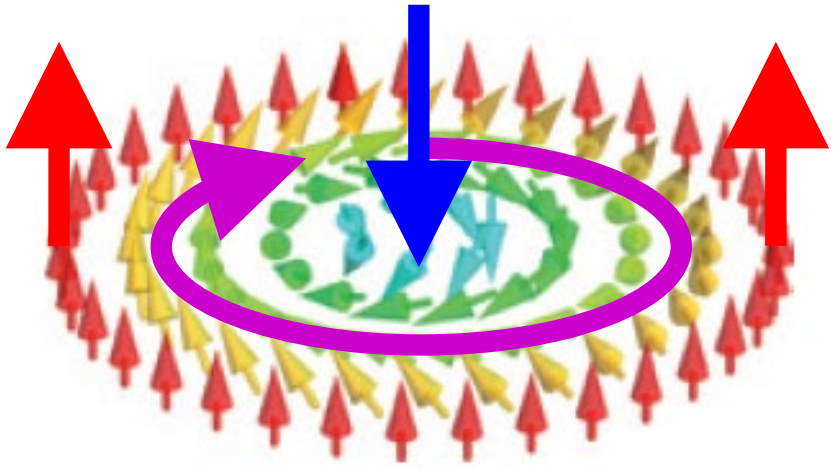

Circularity (CW and CCW)

Polarity (Core-up, Core-down) anti-parallel to perimeter

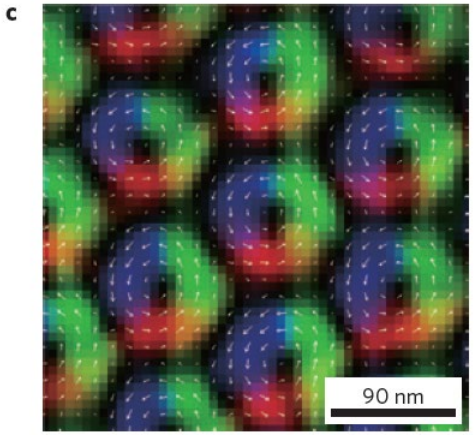

Fert, Cros, Sampaio, Nat. Nanotechnol. **8**, 152 (2013).

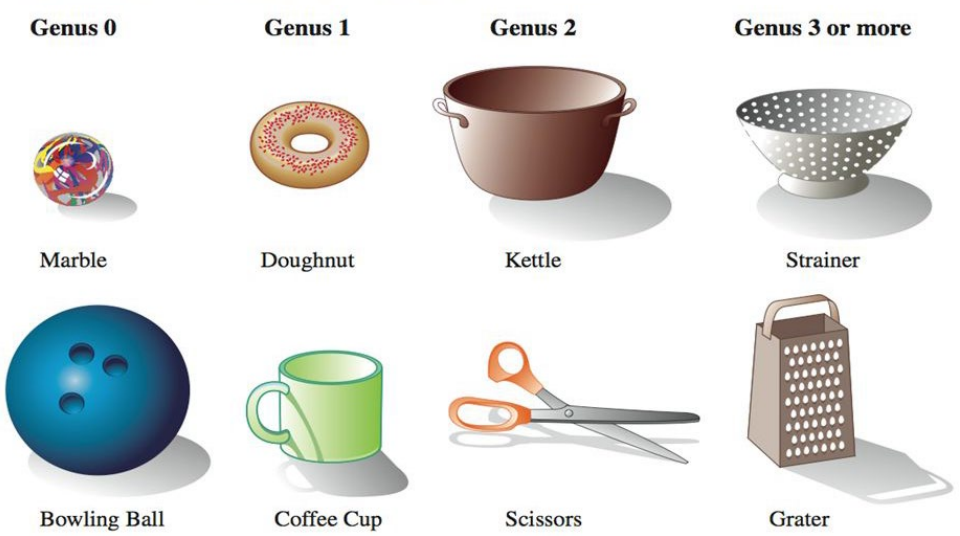

Changing between topological classes requires irreversible processes

Skyrmions: a brief introduction

I. Kezsmarki et al, Nature Materials **volume14**, pages1116–1122 (2015)

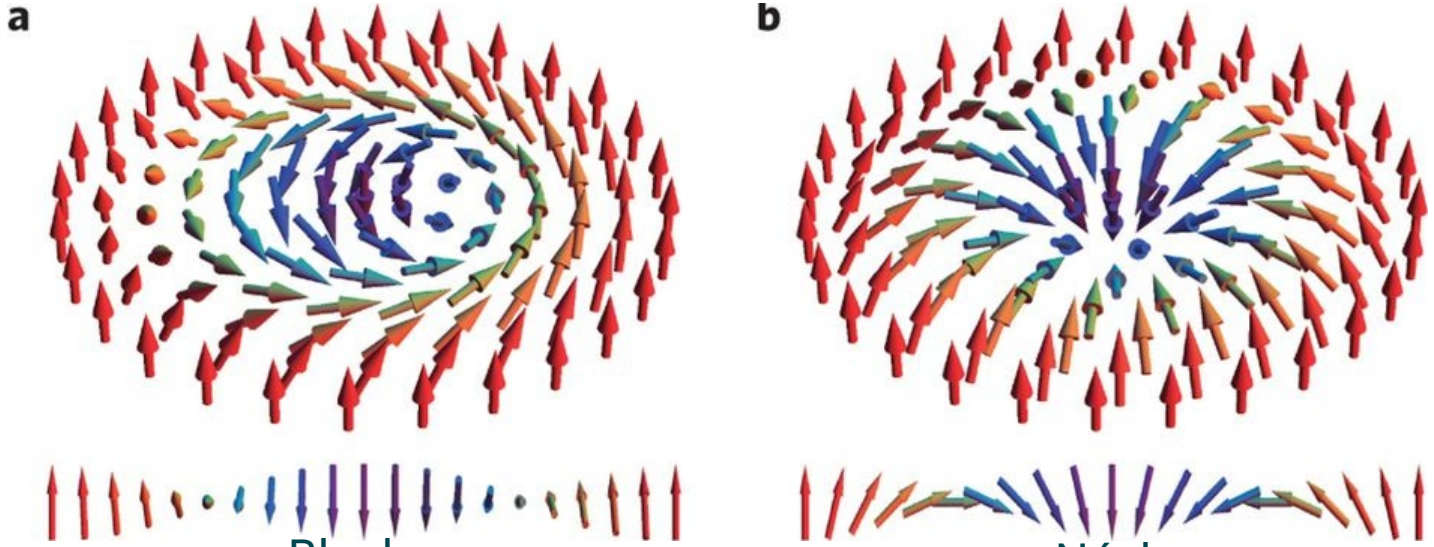

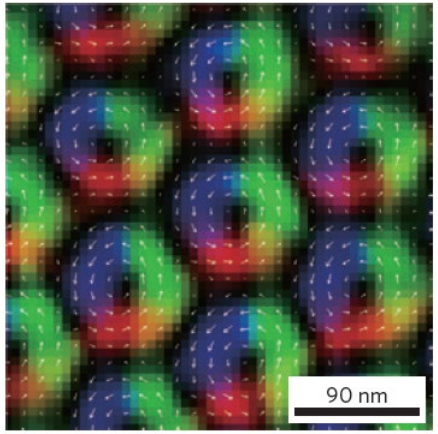

Fert, Nat. Nanotechnol. **8**, 152 (2013).

Fourier Transform

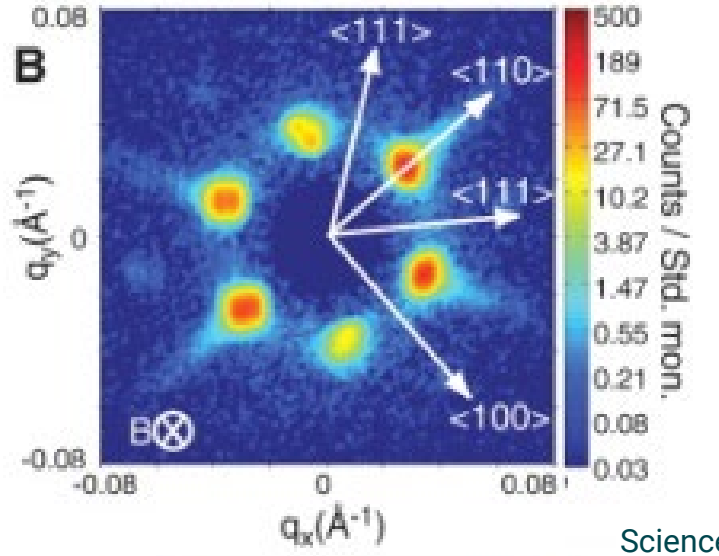

Science 323, 915 (2009)

Frequently form hexagonally packed arrays with long-range ordering

Magnetism effects on Skymrion stability

Science 323, 915 (2009)

Fert, Nat. Nanotechnol. **8**, 152 (2013).

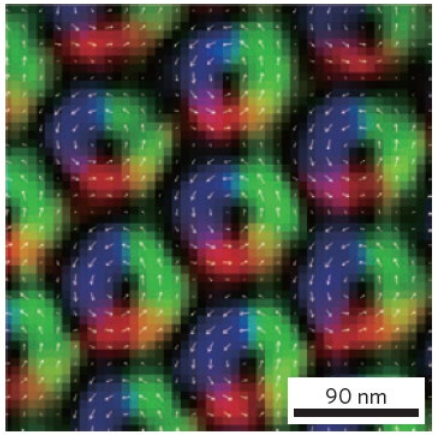

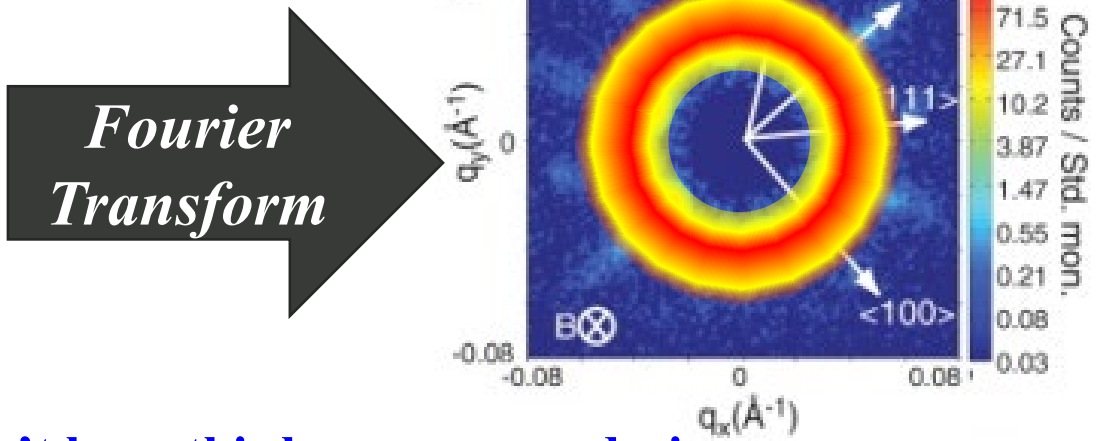

Imagine if we didn't have this long-range ordering…

Origin of the long-range order is in magneto-crystalline coupling

We are interested in skyrmion systems which have weak magnetocrystalline coupling

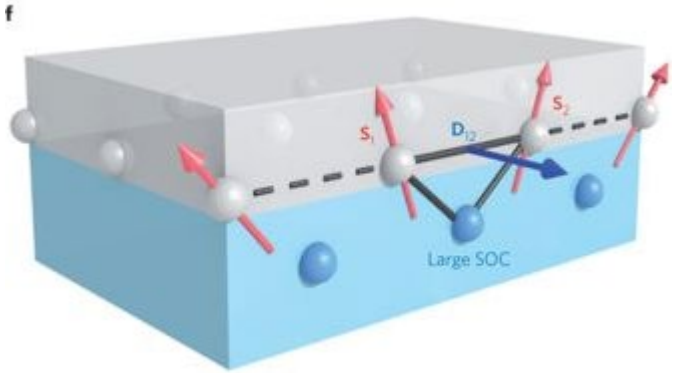

Fert *et al.*, Nat. Nanotechnol. **8**, 152 (2013)

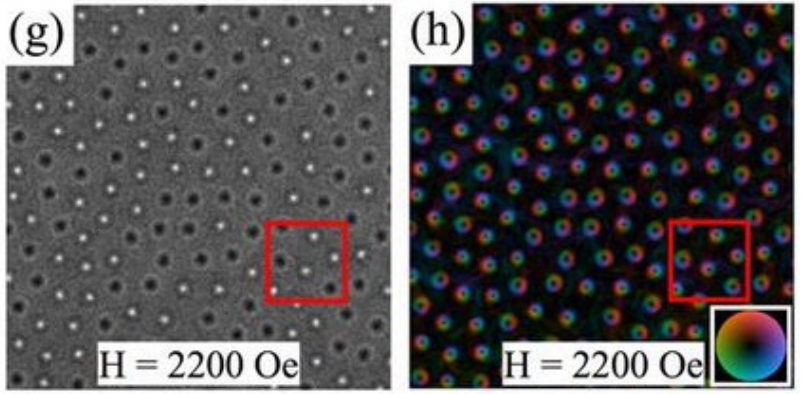

Montoya *et al.*, Phys. Rev. B **95**, 024415 (2017)

OAK RIDGE National Laboratory

Fe/Gd Multilayer Thin Films: The Ingredients for Skyrmions at Ambient Conditions

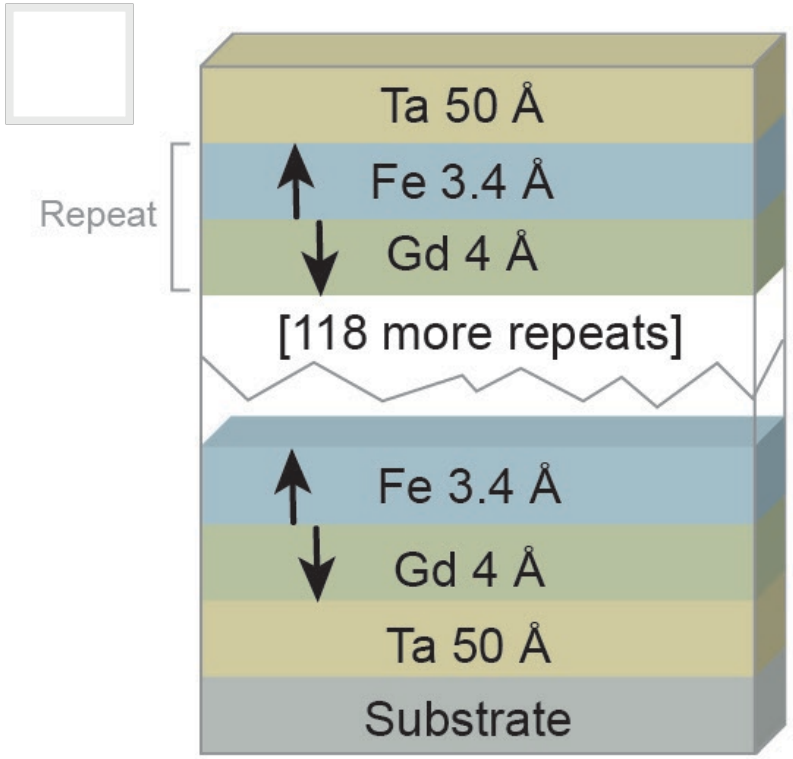

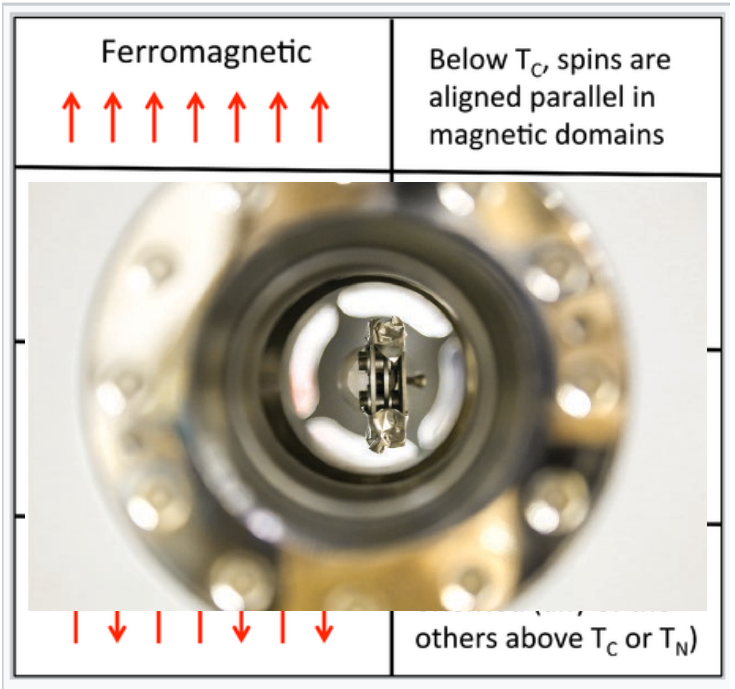

chem.libretext.org

Ferrimagnetic construction with perpendicular magnetic anisotropy

Dipole-stabilized skyrmions

Limited/no DMI

No in-plane structure to cement a long-range orientation

Forming the Skyrmion State

Montoya *et al.*, Phys. Rev. B **95**, 024415 (2017)

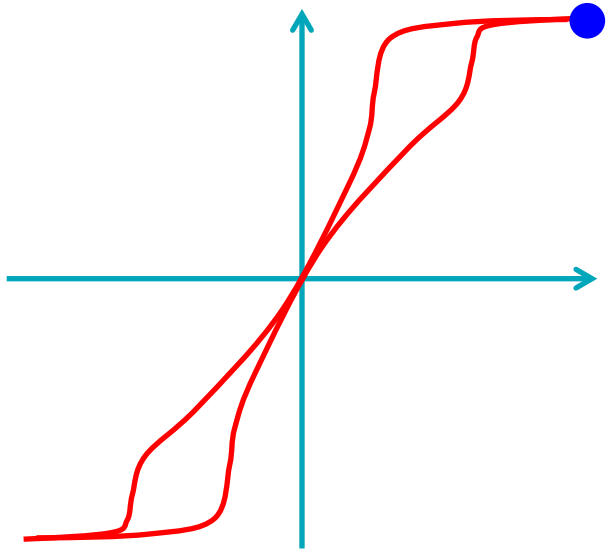

Montoya et al., Phys. Rev. B **95**, 024415 (2017)

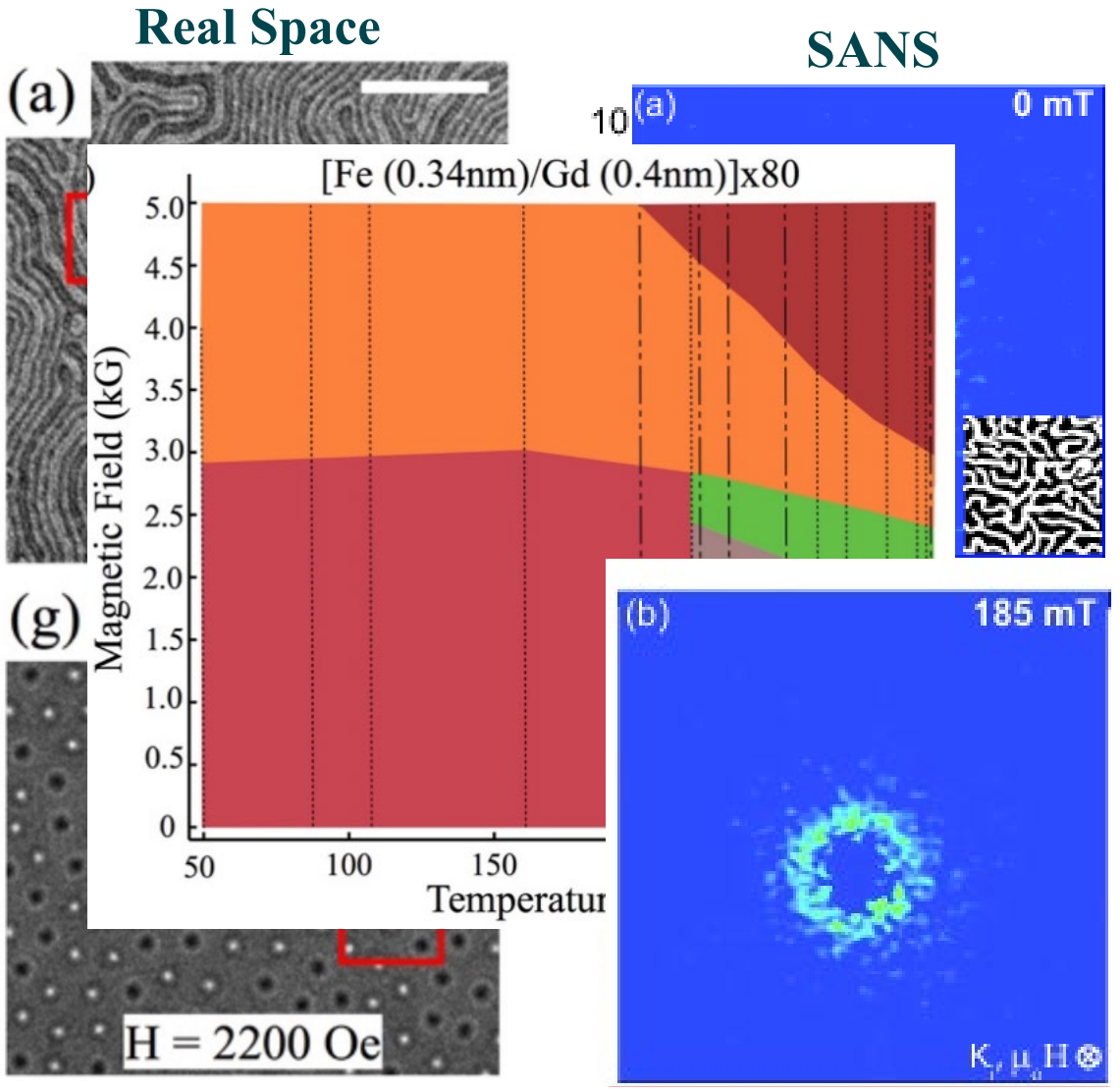

From saturation, worm domain remanent state

Break up into chiral bubbles, no chirality control, no long range order

Generating an Artificial Striped Phase

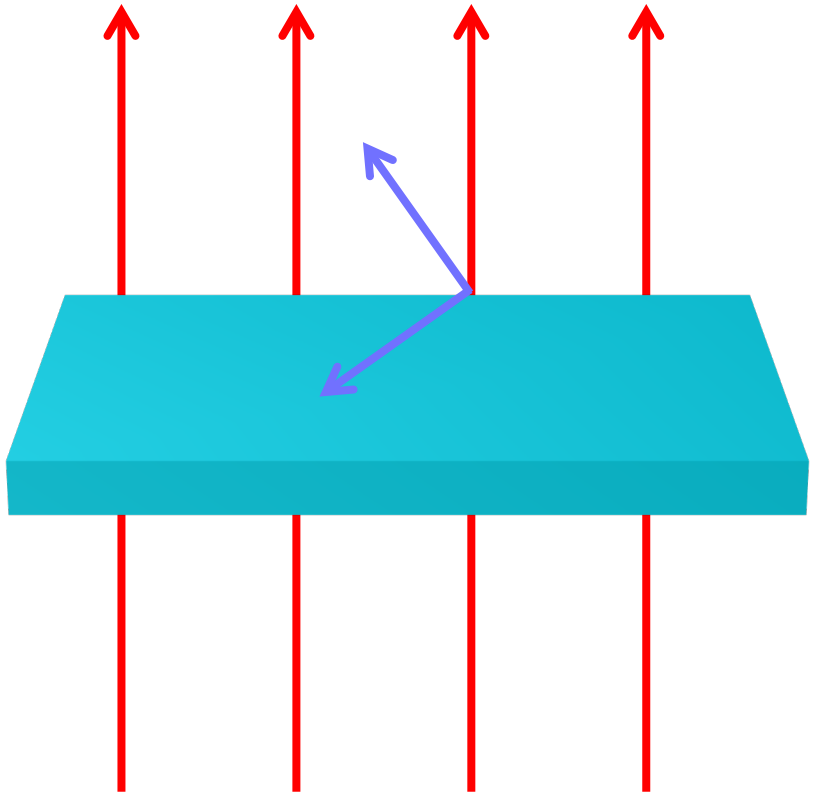

Applied Field

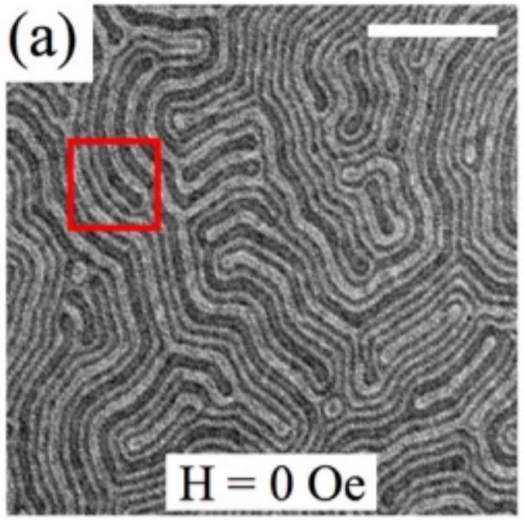

Labyrinth (or worm) domains

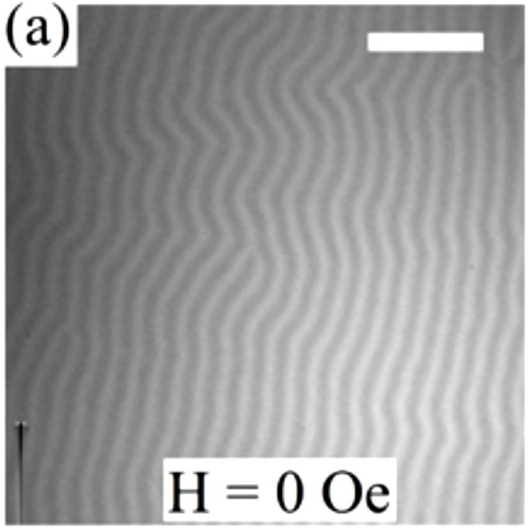

Tilting the sample imparts an in-plane field which breaks the symmetry

Artificial Stripe Domain

Generating an Artificial Striped Phase

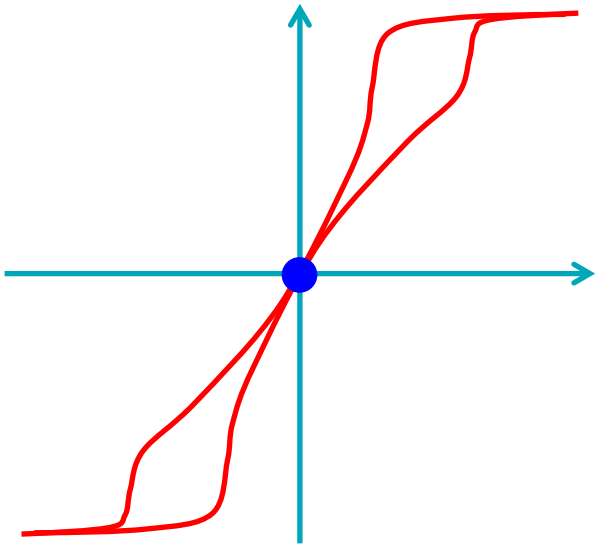

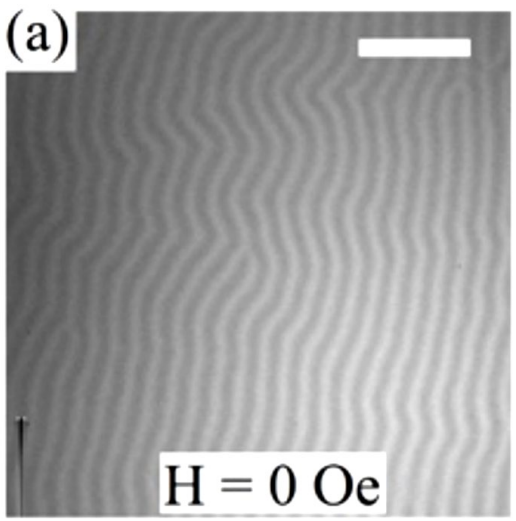

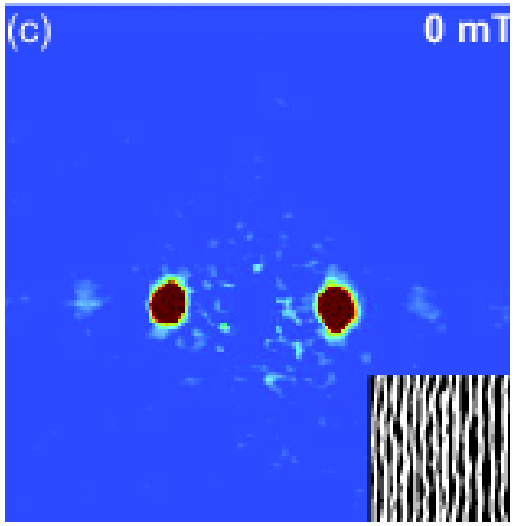

Desautels et al., *Under Review*

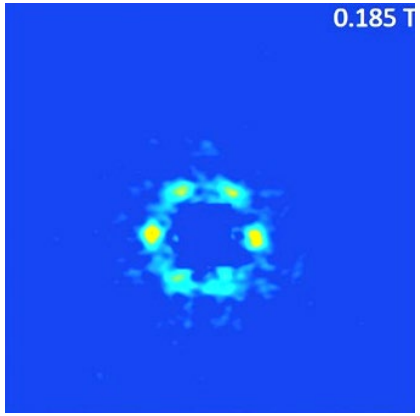

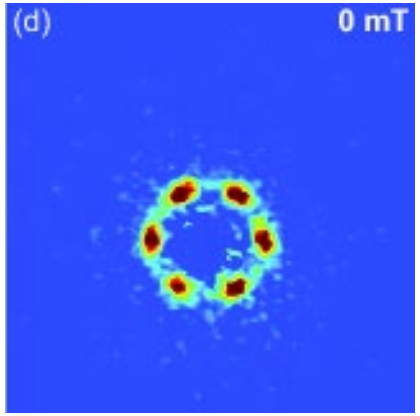

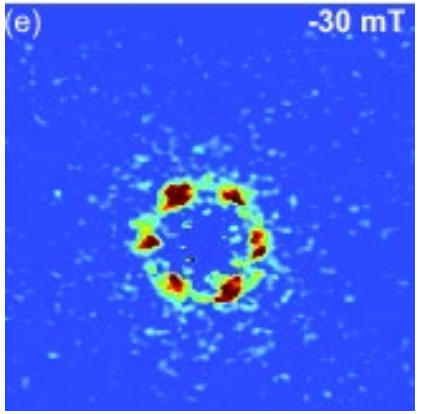

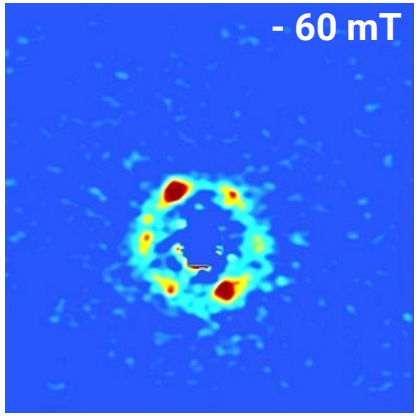

Skyrmion lattice Stability Envelope

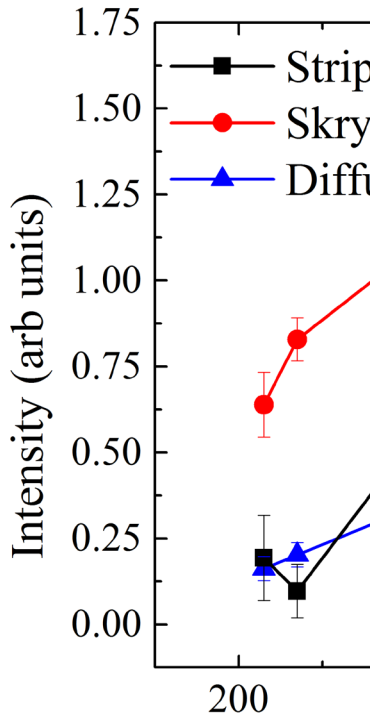

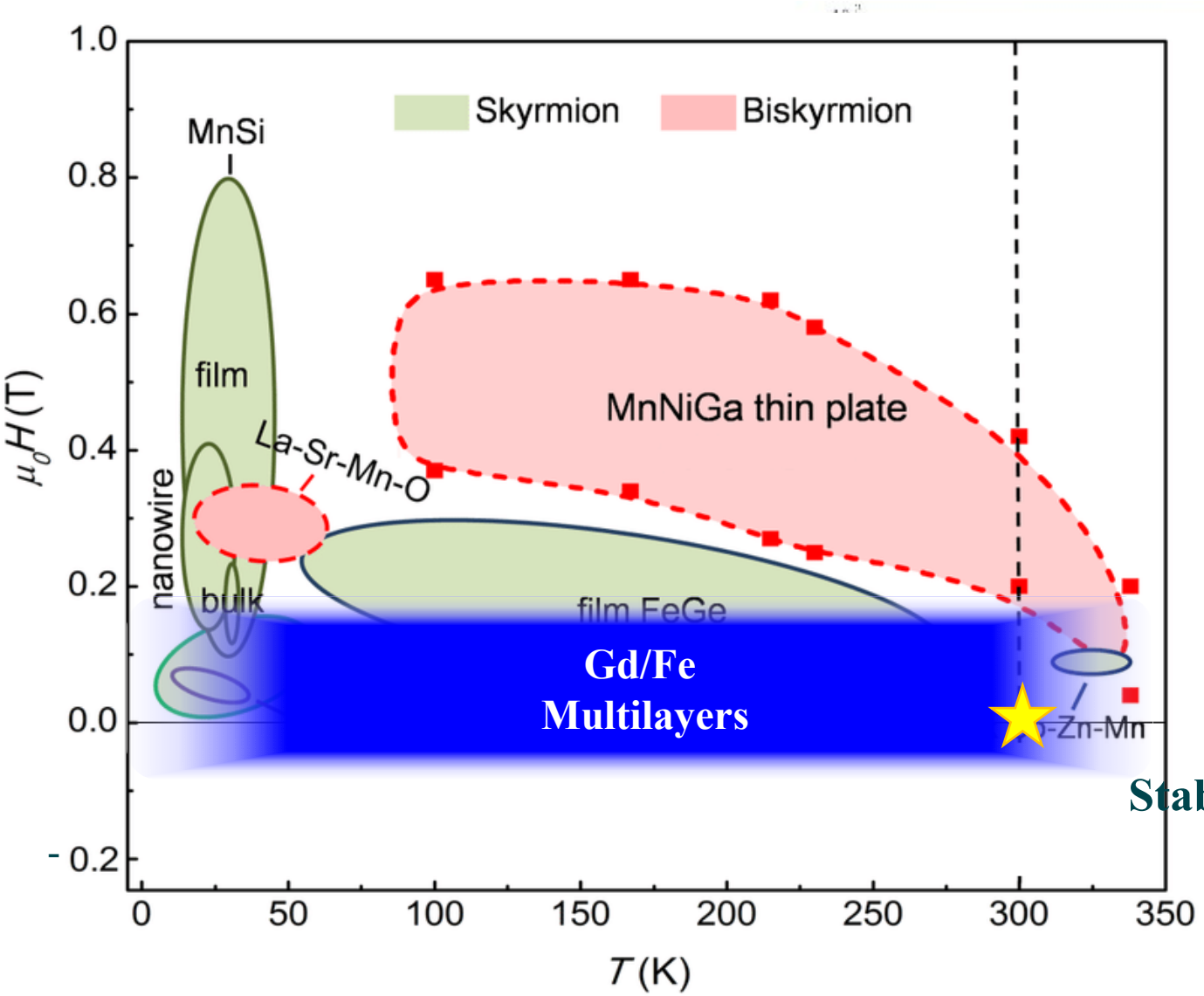

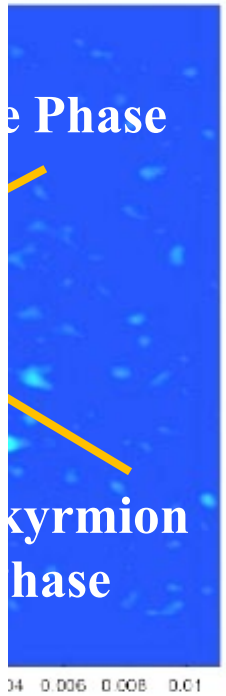

Stable at room temperature and zero field!

Adv. Mater. 28, 6887 (2016)

Implications of Chirality Control on the stability of Skyrmion Lattices

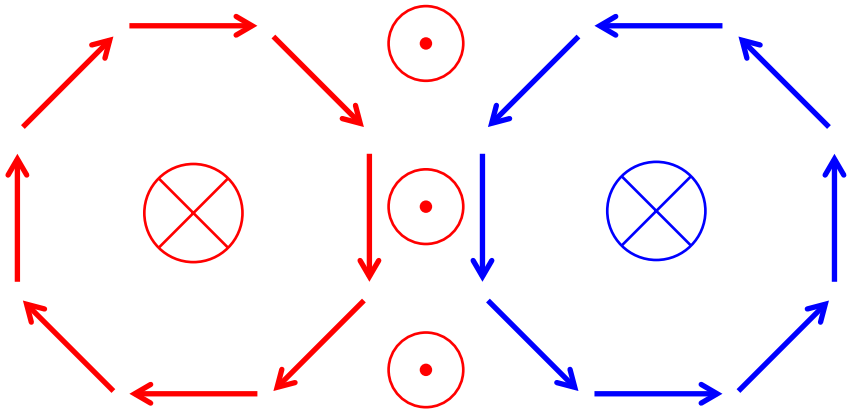

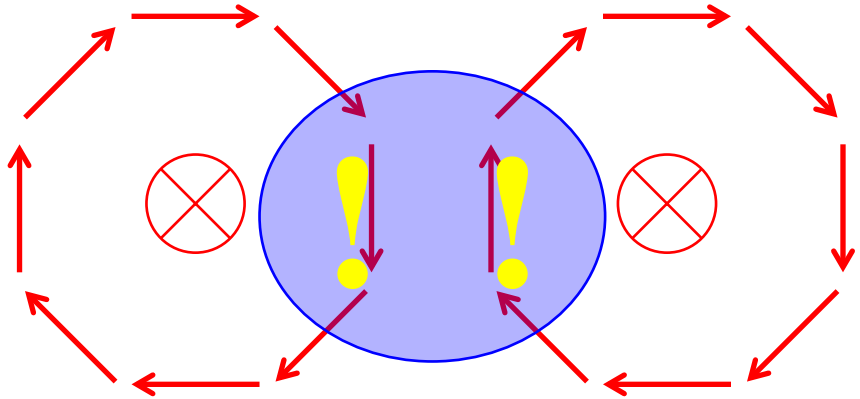

TEM indicates Bloch-type structure with no circularity control

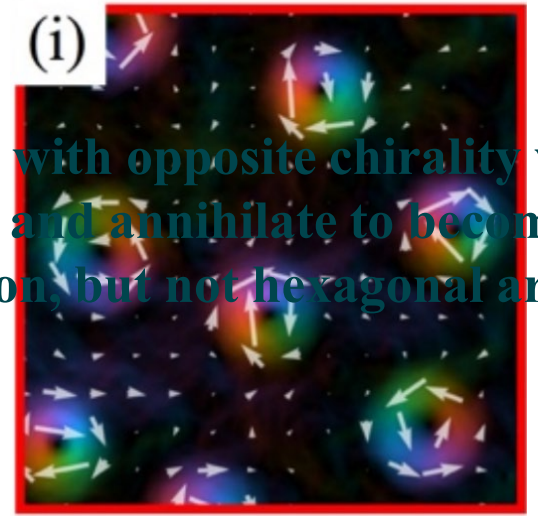

Bubbles with opposite chirality will coalesce and annihilate to become a biskyrmion, but not hexagonal arrays

Strong repulsive interactions between bubbles with identical chirality

→ Hexagonally Ordered Arrays

Implications of Chirality Control on the stability of Skyrmion Lattices

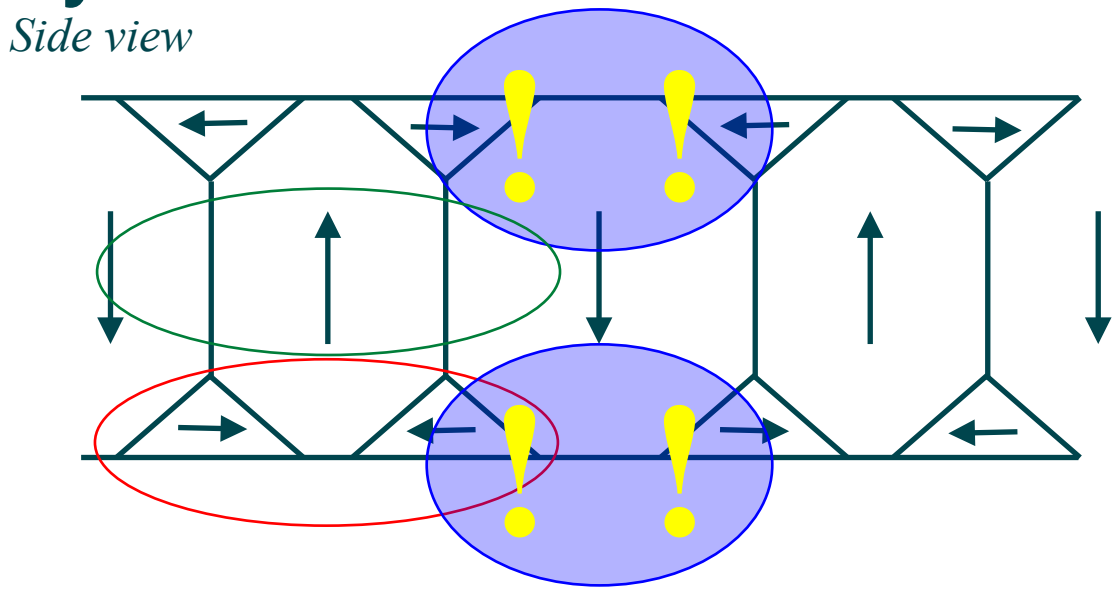

Assumed these are flux-closure domains with no defined chirality

Strong Repulsive Interaction

Repulsive interactions due to surface features, which have their chirality defined by the dipole fields

Appears as Néel Skyrmion, not Bloch (as observed with TEM)

Maybe Neel on the top and bottom, Bloch in the middle

Without DMI, the Bloch region has no net chirality (as observed in TEM)

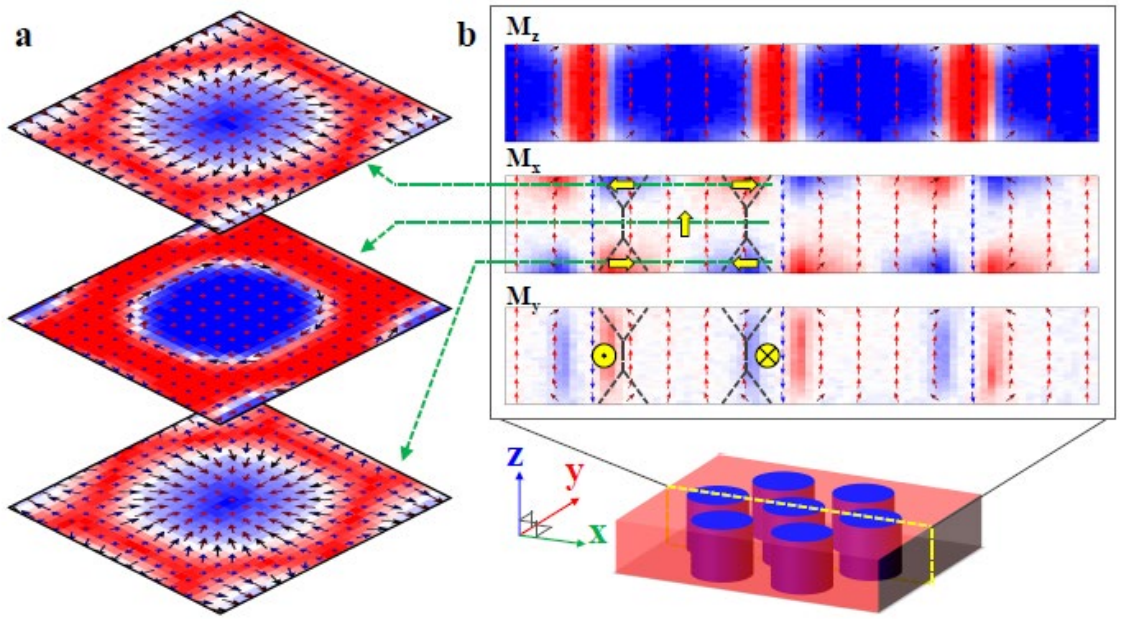

Thin Films studies at GP-SANS

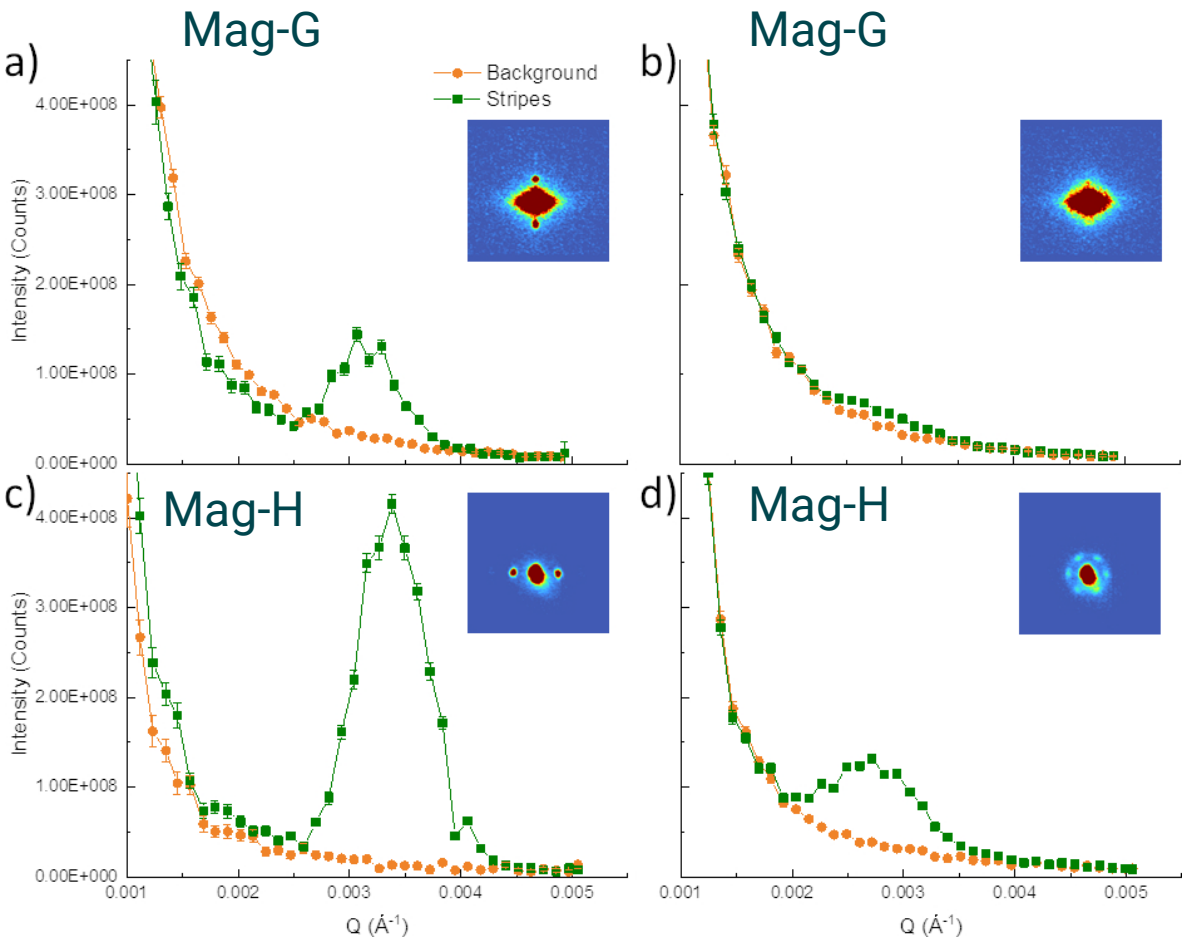

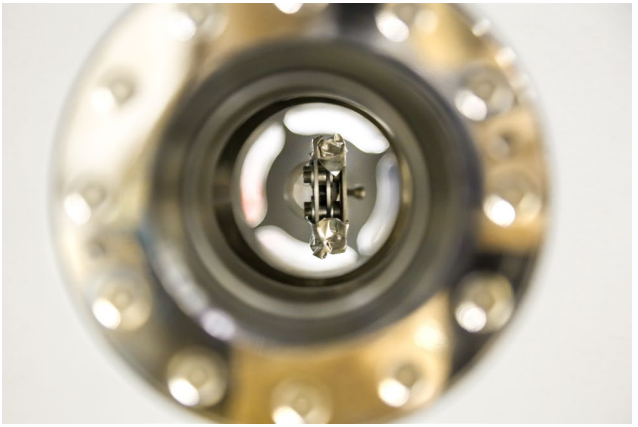

Mag-G

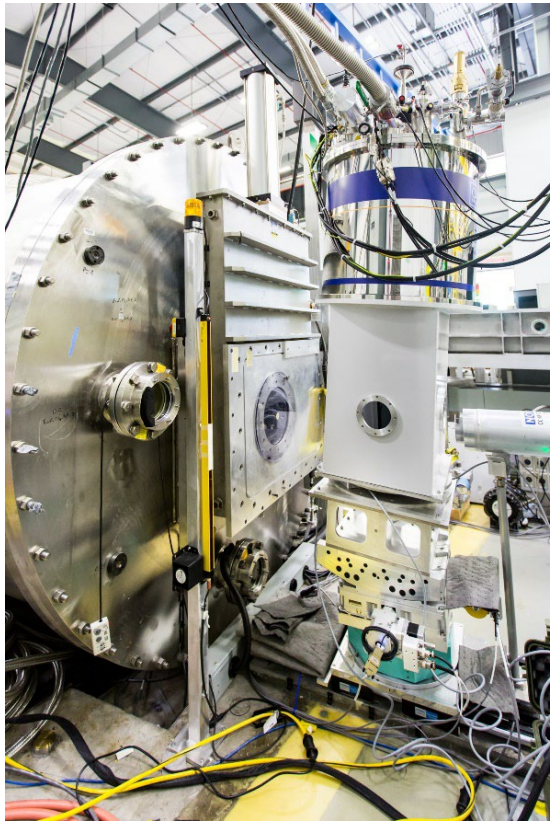

Mag-H

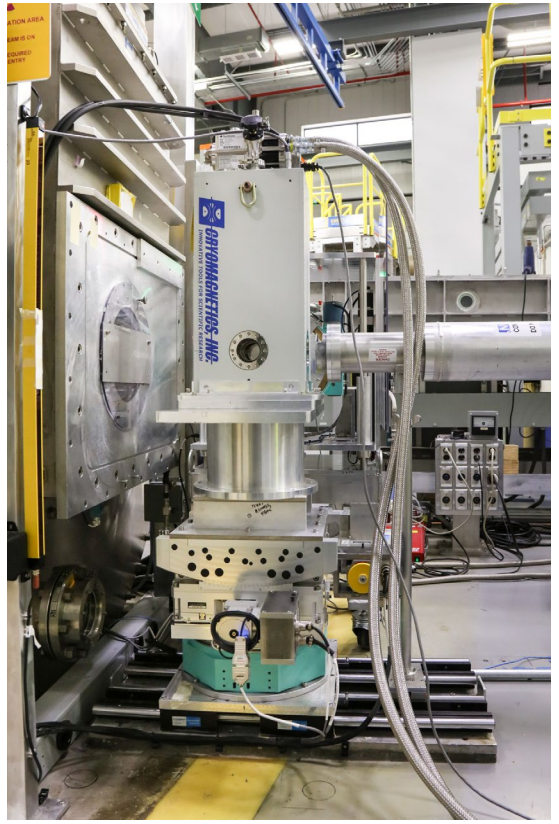

OAK RIDGE National Laboratory

Use of Small-Angle Neutron Scattering to Characterize Novel Steels for Reactor Applications

Kevin G. Field[1], Kenneth C. Littrell[1*], and Samuel A. Briggs[2]

[1]*Oak Ridge National Laboratory*

[2]*Sandia National Laboratories*

U.S. DEPARTMENT OF ENERGY

ORNL IS MANAGED BY UT-BATTELLE LLC
FOR THE US DEPARTMENT OF ENERGY

AFC Advanced Fuels Campaign

Oxidation of cladding is key towards core degradation during a coolant-limited accident scenario

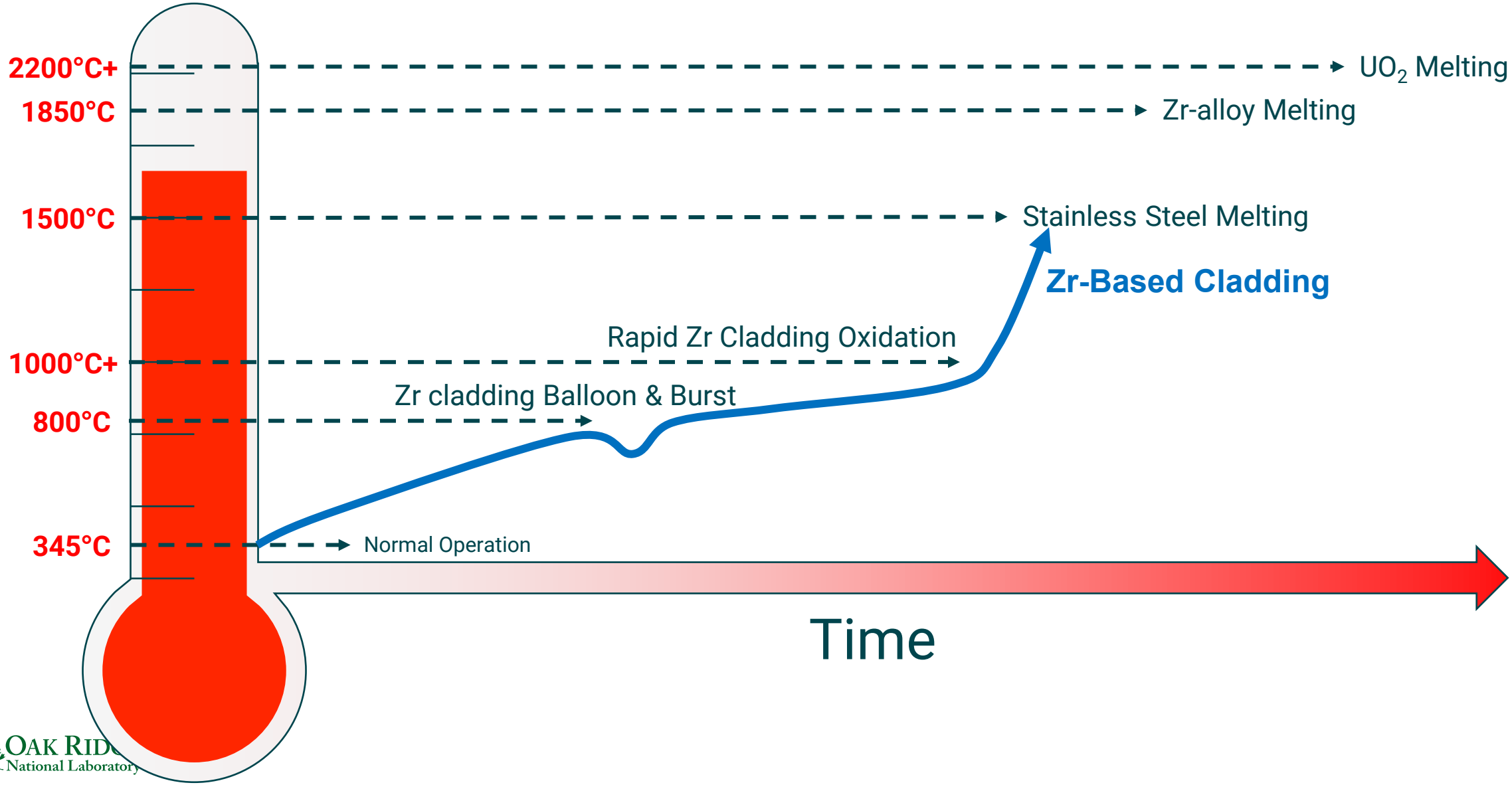

Oxidation of cladding is key towards core degradation during a coolant-limited accident scenario

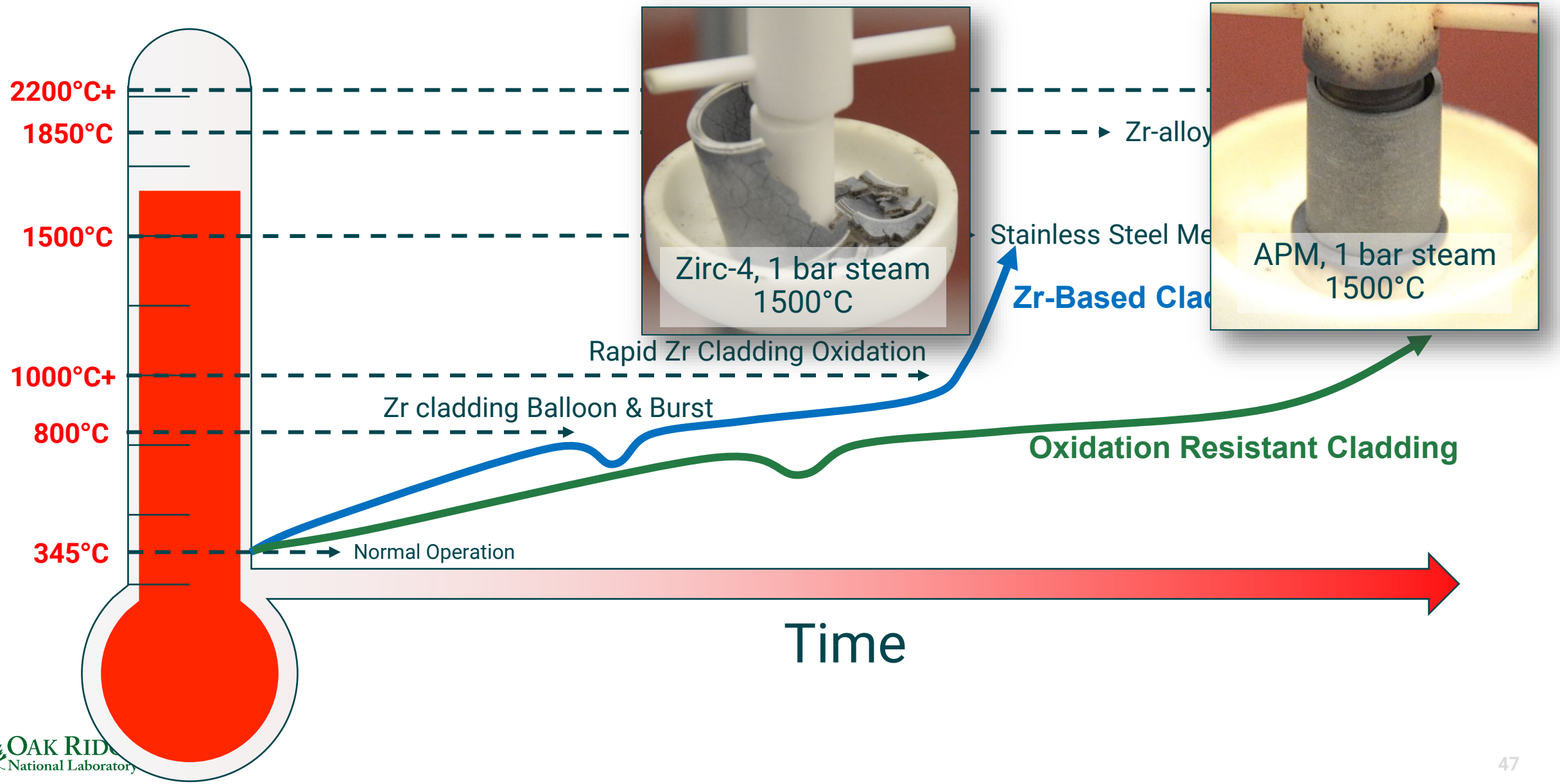

SANS Scattered Intensity: Local Monodispersed Approximation[1]

$$\frac{d\sigma}{d\Omega}(q) = \Delta\rho^2 \int_0^\infty \phi(q,R)^2 S[q, R_{HS}(R)] N(R)\, dR + Aq^{-B} + C$$

- Contrast: $\Delta\rho^2 = \left(\rho_{particle} - \rho_{matrix}\right)^2$
- Form factor (for spheres):

$$\phi(q,R) = 3V_o[\sin(qR) - qR\cos(qR)]/(qR)^3$$

- Structure factor: $S[q, R_{HS}(R)] = [1 + 24\eta_{HS} G(R_{HS}q)/(R_{HS}q]^{-1}$
- Size distribution (Weibull density function): $N(R) = (R/\bar{R})^{b-1} exp[-(R/\bar{R})^b]$
- Low-q power-law: Aq^{-B}
- Background: C

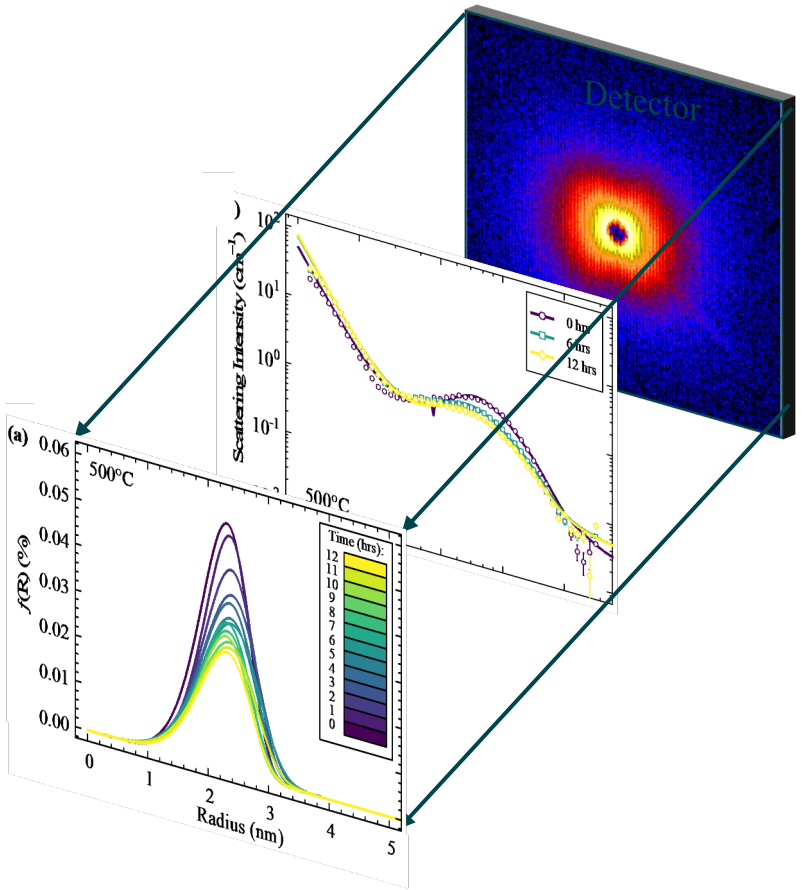

J.S. Pedersen, Determination of Size Distributions from Small-Angle Scattering Data for Systems with Effective Hard-Sphere Interactions, *J. Appl. Cryst.*, **27**, pgs. 595-608, 1994.

Magnetic Shielded-SANS measurements : Contrast from Neutrons

1. ***Nuclear contrast:***

$$\Delta\rho_{nucl}^2 = \left(\rho_{nucl,particle} - \rho_{nucl,matrix}\right)^2$$

2. ***Magnetic contrast:***

$$\Delta\rho_{mag}^2 = \left(\rho_{mag,particle} - \rho_{mag,matrix}\right)^2$$

$$\frac{d\sigma}{d\Omega}(q) = \Delta\rho^2 \int_0^\infty \phi(q,R)^2 \ldots[]$$

$$\left[\Delta\rho_{nucl}^2 + \Delta\rho_{mag}^2 sin^2\alpha\right]$$

Can exploit magnetization to extract composition

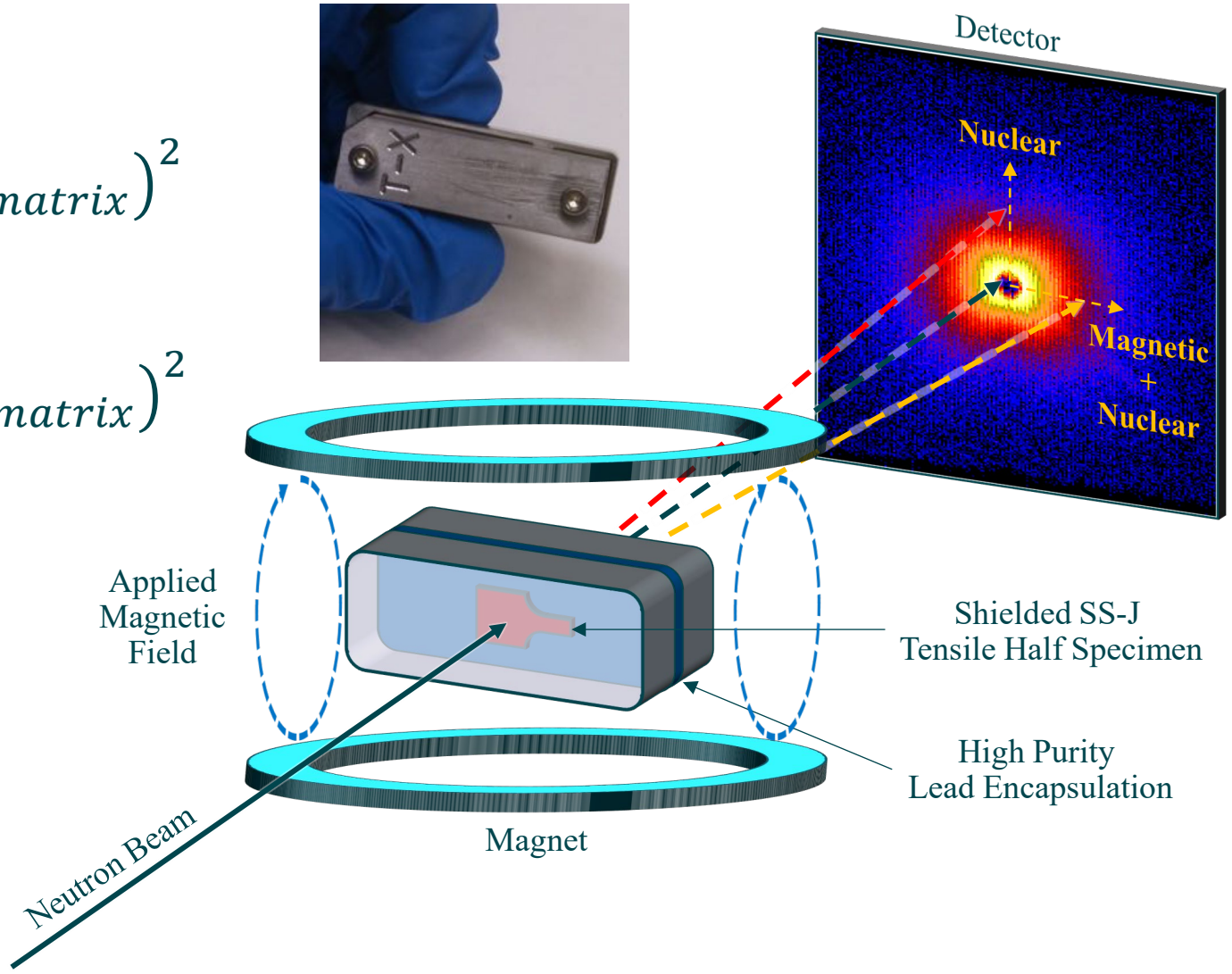

Radiation tolerance of FeCrAl alloys is analogous to FeCr alloys under similar irradiation conditions

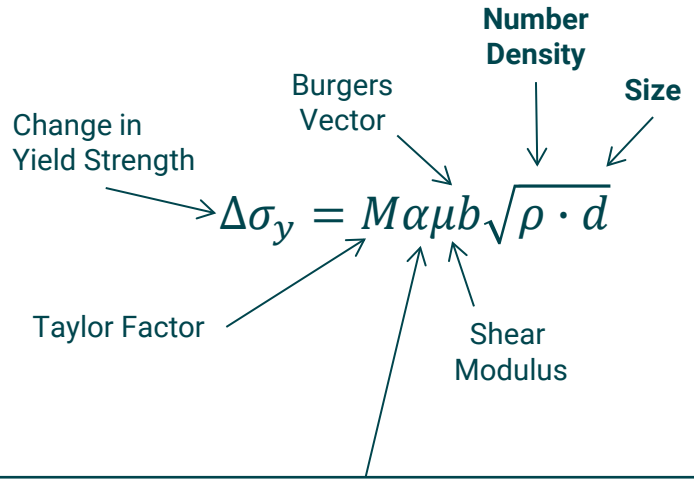

Super. rule	Barrier strength of visible defects (α)			
	Cr-rich α'	⟨100⟩	½⟨111⟩	Line
Linear	0.04	0.31	0.05	0.68
SRS	0.06	0.33	0.17	0.56

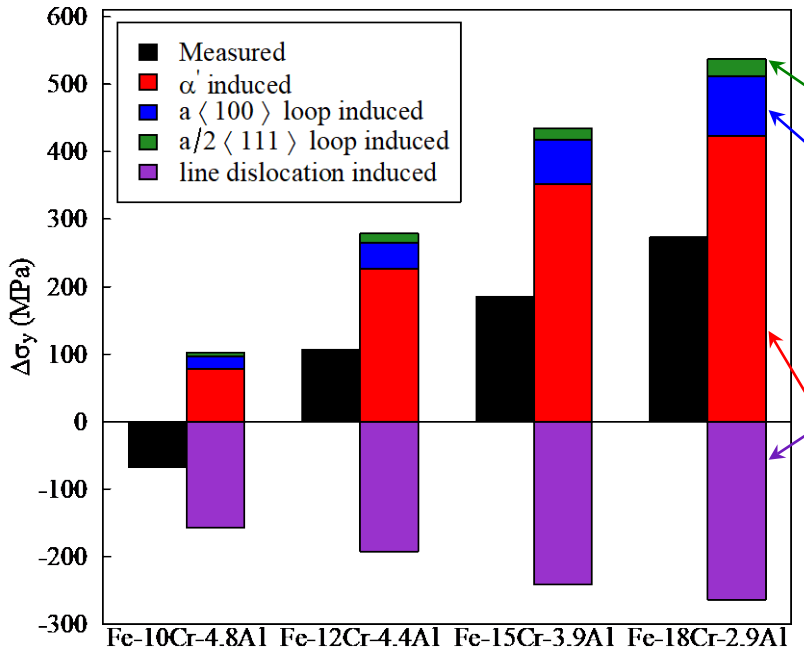

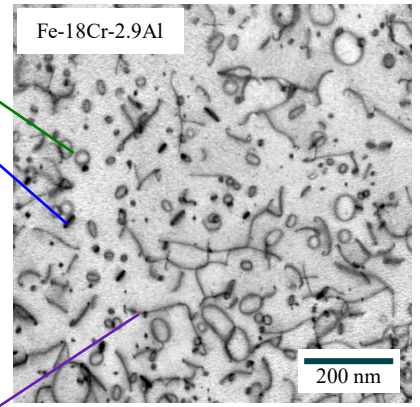

STEM image showing dislocation loops and line dislocations in 1.8 dpa, 382°C irradiated Fe-18Cr-2.9Al alloy

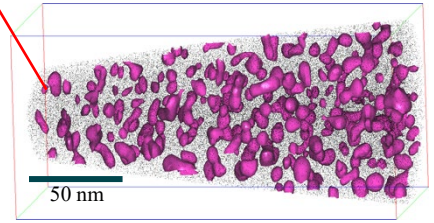

APT reconstruction showing α' in 1.8 dpa, 382°C irradiated Fe-18Cr-2.9Al alloy

- Dispersed barrier hardening (DBH) has linked radiation-hardening in FeCrAl alloys to formation of Cr-rich α' and dislocation loops after neutron irradiation to 1.8 dpa at 382°C

Need exists to understand the role of composition and temperature on the formation and progression of Cr-rich α' in FeCrAl alloys

[1] K. G. Field, X. Hu, K. C. Littrell, Y. Yamamoto, L. L. Snead, Radiation tolerance of neutron- irradiated model Fe-Cr-Al alloys, *Journal of Nuclear Materials*, **465**, pgs. 746-755, 2015.

A large amount of FeCrAl samples have been irradiated and/or tested over the past 5 years…

…how do we characterize α′ from these efficiently?

Magnetic Shielded-SANS measurements: Role of temperature and composition on α′

- Selected FeCrAl alloys irradiated in HFIR to determine temperature, composition, and microstructure trends

Capsule ID	Number Samples	Neutron Flux (n/cm^{2}s) E > 0.1 MeV	Neutron Fluence (n/cm^2) E > 0.1 MeV	Dose Rate (dpa/s)	Dose (dpa)	Irradiation Temperature (°C)
FCAT-01	45	1.10×10^{15}	2.17×10^{21}	9.6×10^{-7}	1.9	194.5 ± 37.9
FCAT-02	45	1.04×10^{15}	2.05×10^{21}	9.1×10^{-7}	1.8	362.7 ± 21.2
FCAT-03	45	1.10×10^{15}	2.17×10^{21}	9.6×10^{-7}	1.8	559.4 ± 28.1

Increasing Temp.

- Measurements performed at CG-2 general purpose SANS beamline at HFIR
- Data collected on broken tensile heads in magnetic shielded SANS configuration

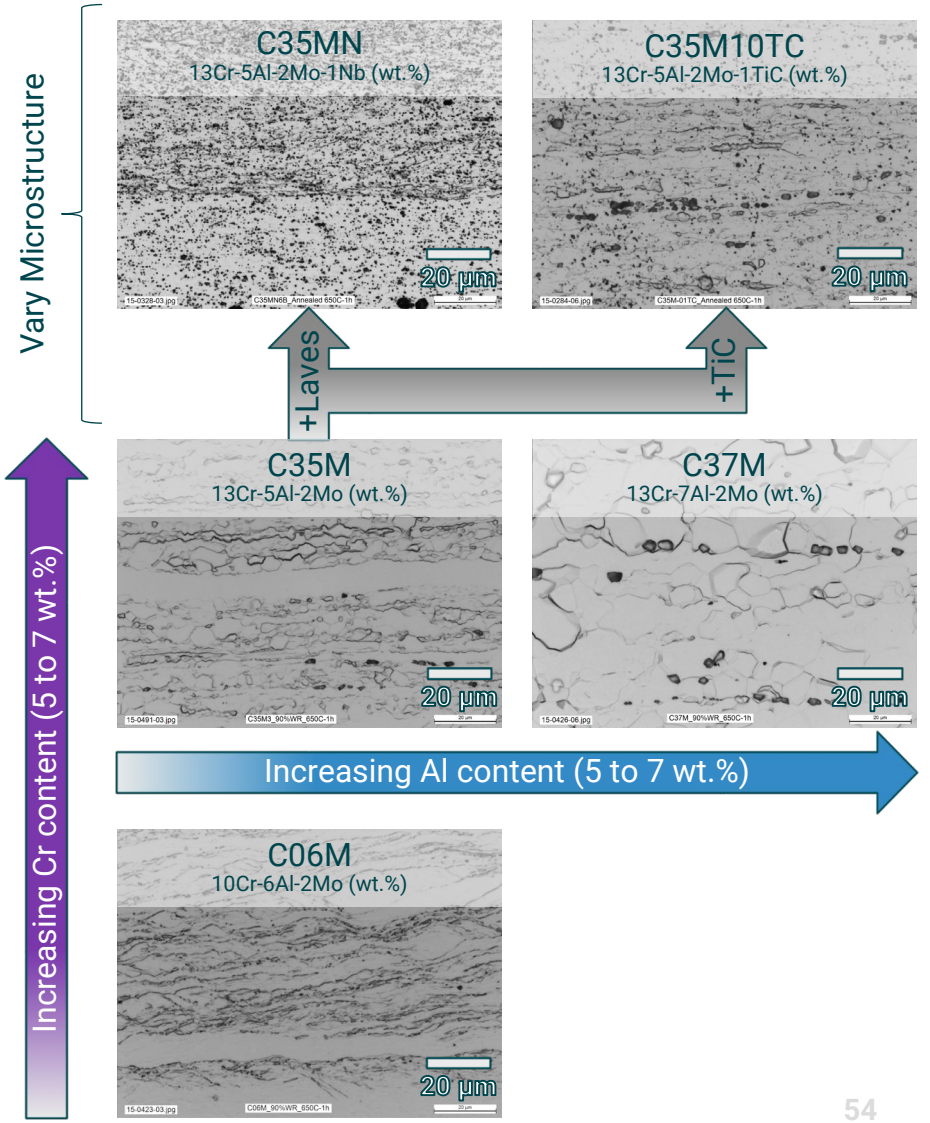

Magnetic Shielded-SANS measurements: Role of temperature and composition on α′

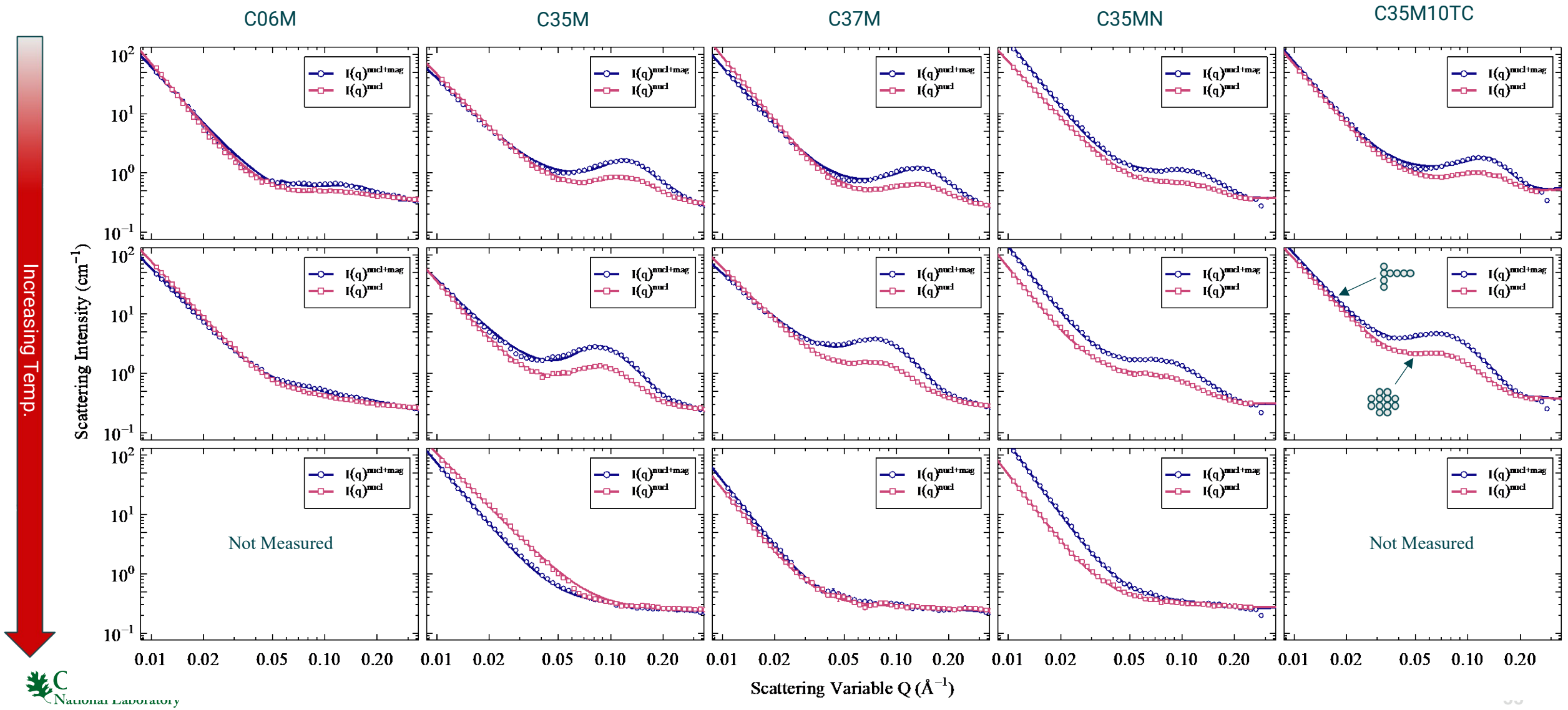

Magnetic Shielded-SANS measurements: Role of temperature and composition on α′

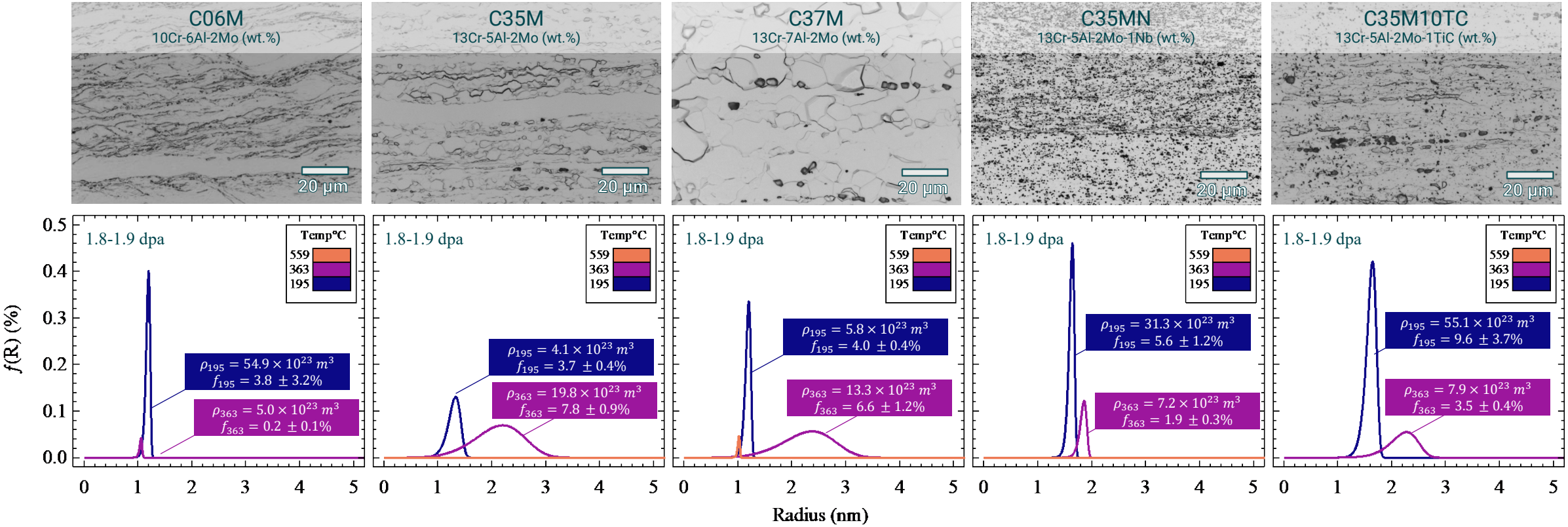

- Increasing irradiation temperature increases mean radius and distribution width
- Cr stronger than Al in control in α' precipitation
- Microstructure (precipitates/grain size) can play a role in α' precipitation

Magnetic Shielded-SANS measurements: Role of temperature and composition on α′

$$\frac{d\sigma}{d\Omega}(q) = \Delta\rho^2 \int_0^\infty \phi(q,R)^2 \ldots []$$

$$\left[\Delta\rho_{nucl}^2 + \Delta\rho_{mag}^2 sin^2\alpha\right]$$

$$A - ratio = \frac{\Delta\rho_{mag+nucl}^2}{\Delta\rho_{nucl}^2}$$

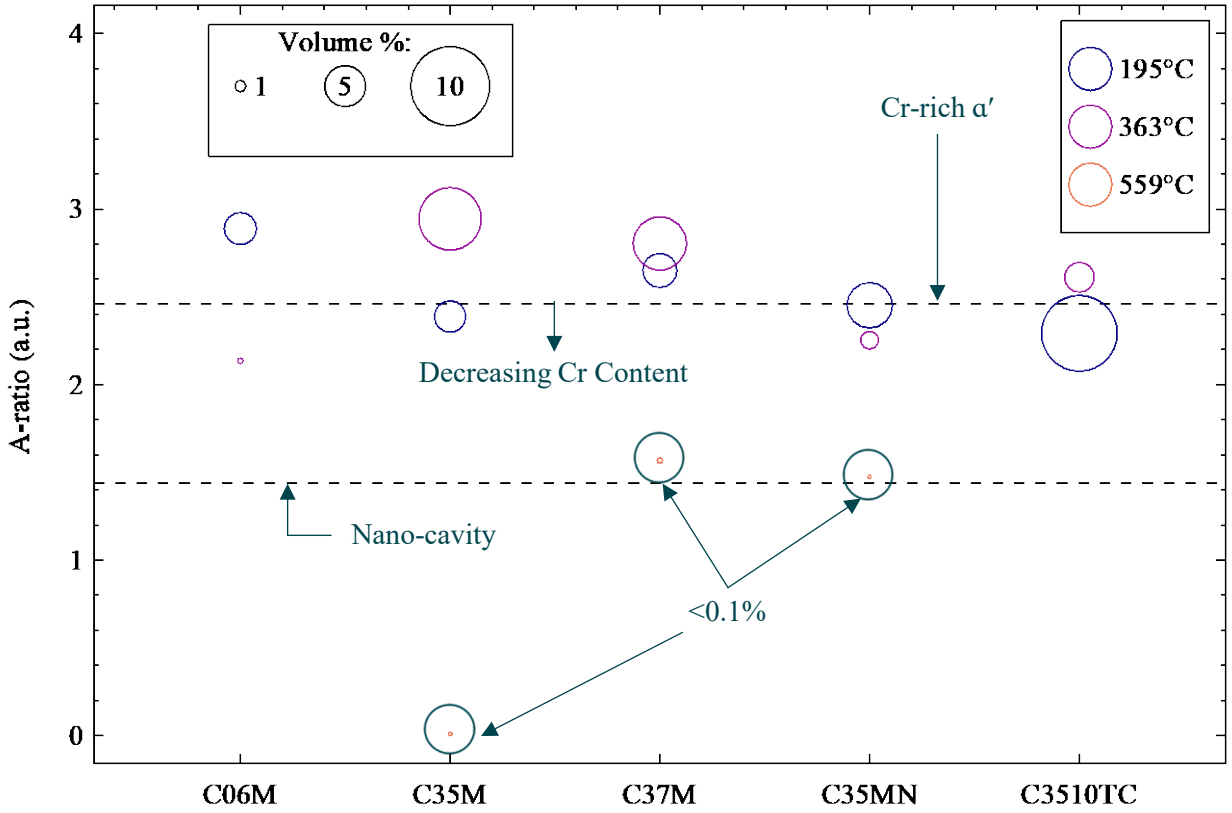

- Magnetic shielded SANS reveals that irradiations below 500°C form primarily α'
  - Typically lower Cr content in 195°C irradiations
- Above 500°C, scattering could be from nano-cavity formation

Practical Application of Ex-situ SANS results:
α′ concern for normal operation, but can be tuned

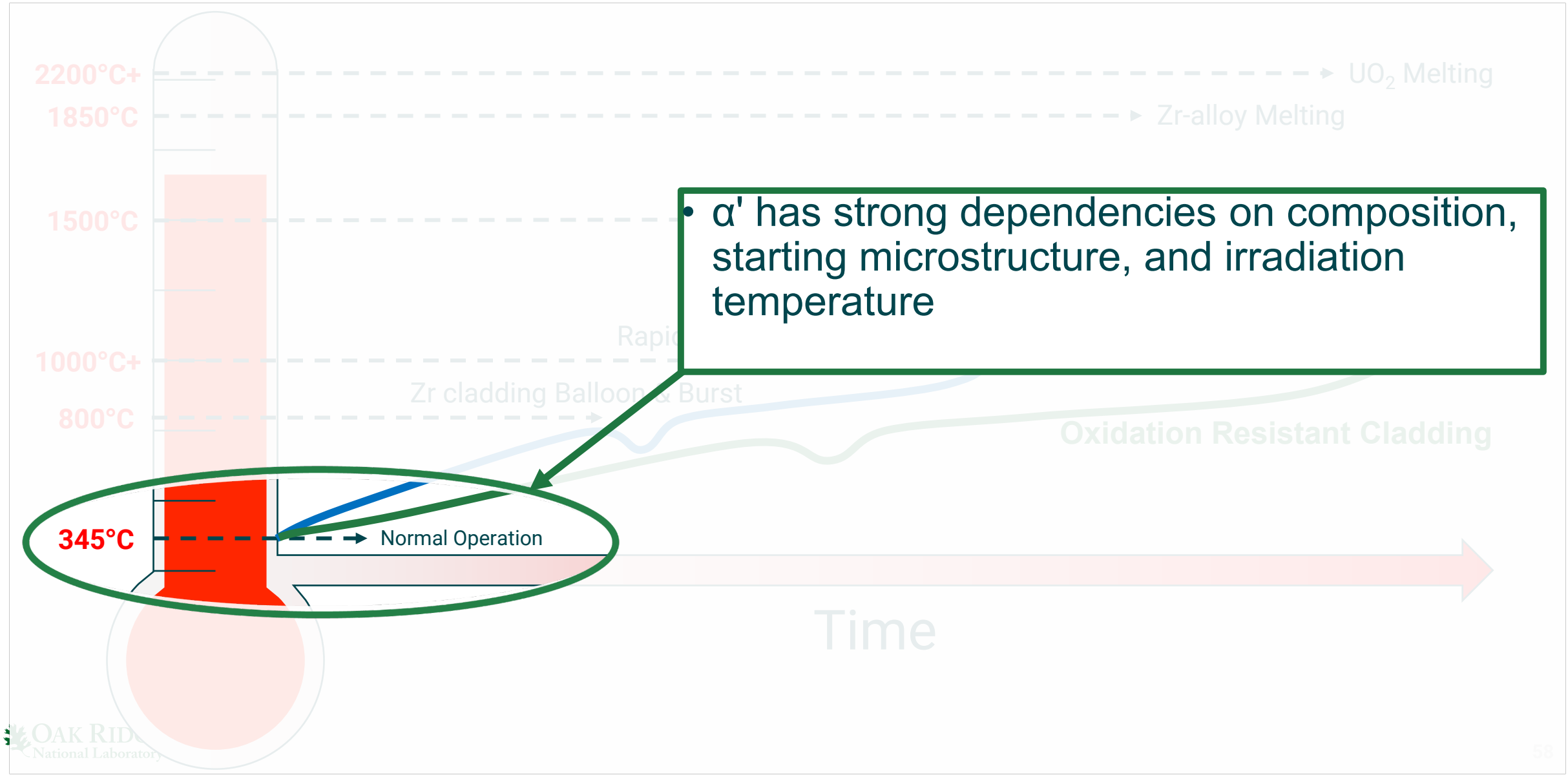

- α' has strong dependencies on composition, starting microstructure, and irradiation temperature

New Directions with SANS

Time-resolved SANS

GI-SANS

Time-resolved SANS (TR-SANS)

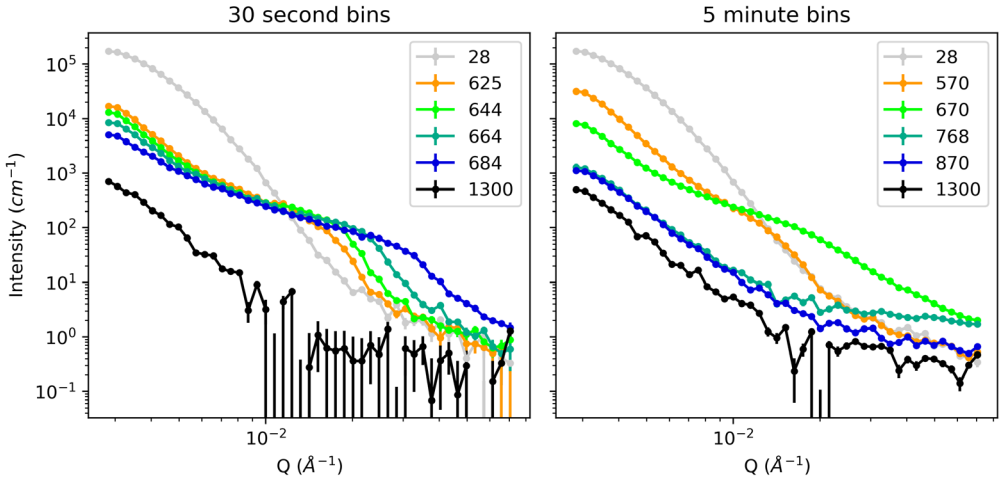

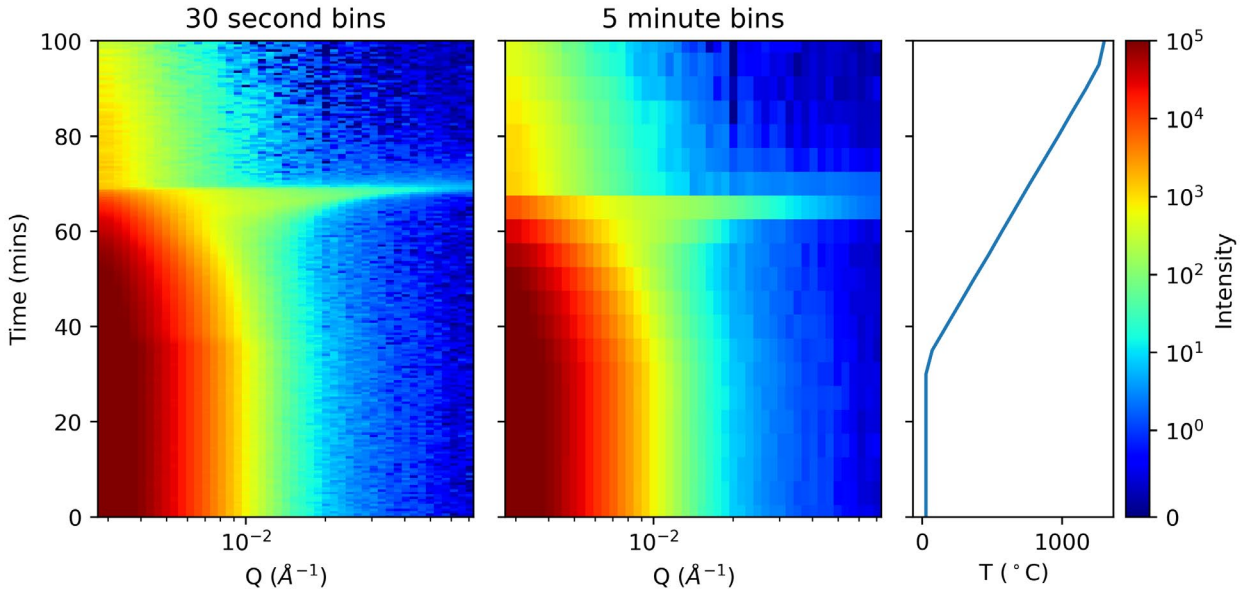

- Additively manufactured reactor steels
- Data(above) collected during ramping temperature in a vacuum furnace.
- Post-processing software can re-bin the data either by time or log value(magnetic field)

- Data collected during magnetic field ramp from 0 to 10 T
- Data sliced by 30 second slices as the field is ramped.

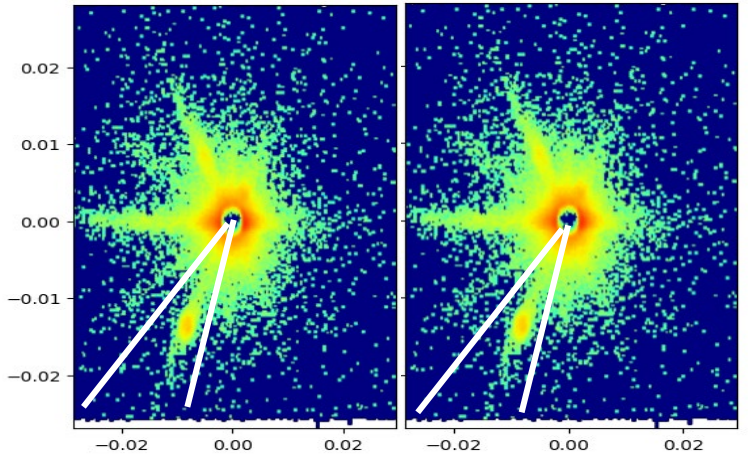

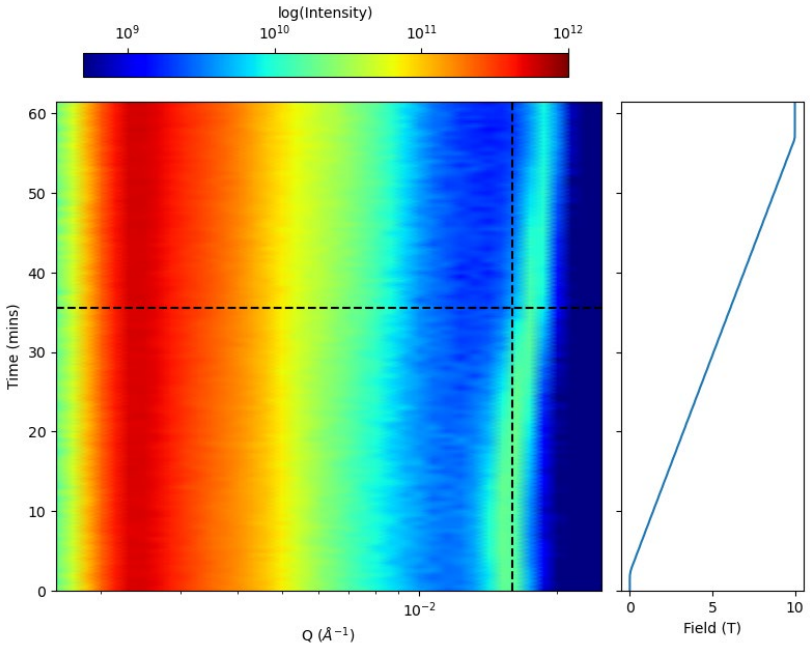

OAK RIDGE National Laboratory

GI-SANS

- Being developed at ORNL at EQ-SANS but GP-SANS, BIO-SANS can do this technique.
- Measuring the specular and off-specular versus sample angle encodes both in-plane and out-of-plane structure of the systems.

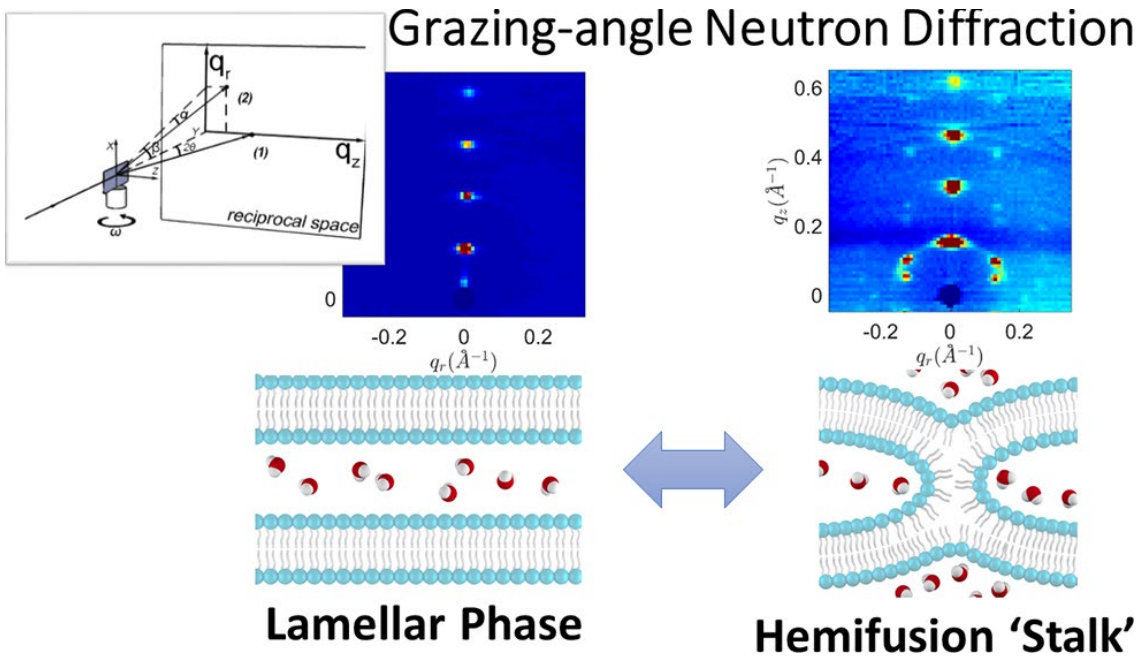

S. Qian and D. K. Rai J. Phys. Chem. Lett. 2018, 9, 5778-5784

Fe/Gd multilayers measured with a large (195 mT) out-of-plane field in the skyrmion phase

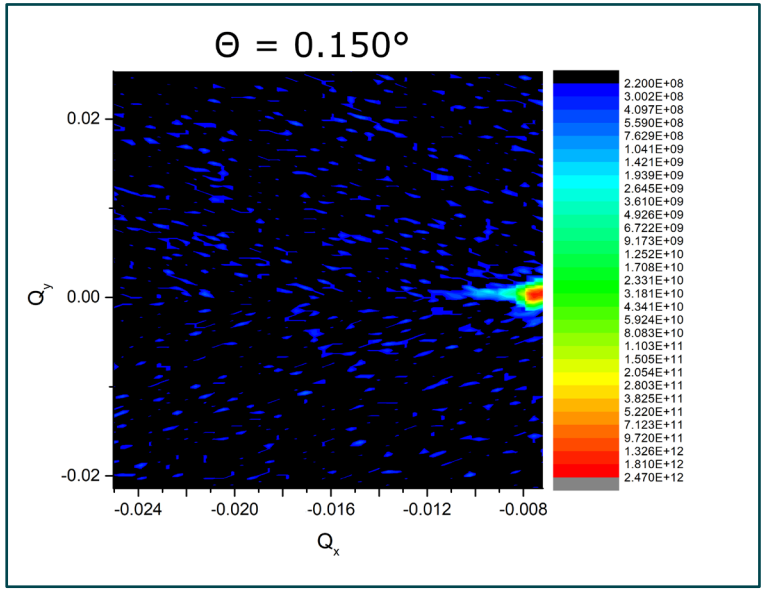

WLNC Liyanage *et. al* Phy. Rev. B **107**, 184412 (2023)

Experts at ORNL on GI-SANS:

- William Heller
- Changwoo Do
- Valeria Lauter

Thank you for your attention.

Neutron Scattering Society of America

ORNL neutron website

- Probes bulk structures from 0.1 nm – 1 μm
- Contrast tuning with isotopes & magnetism
- Works with diverse sample environments
- Applies across soft matter, magnetism, and alloys

Instrument Teams:

GP-SANS


Lisa DeBeer-Schmitt

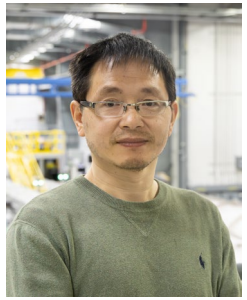
Lilin He


Karin Bichler


Arina Rostopchina

Bio-SANS


Venky Pingali

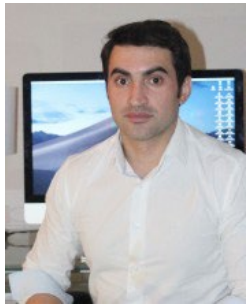
Wellington Leite


Volker Urban


Felicia Gilliland

USANS


Wei-ren Chen


Gernot Rother


Yingrui Shang

EQ-SANS


Carrie Gao


Changwoo Do


William Heller


Gergely Nagy

OAK RIDGE National Laboratory

NXS Lecture - Lisa DeBeer-Schmitt

"Small Angle Neutron Scattering"

Extra slides

OAK RIDGE
National Laboratory

ORNL IS MANAGED BY UT-BATTELLE LLC
FOR THE US DEPARTMENT OF ENERGY